Chapter 7

Phase Diagram of The Ternary BaO-Bi_2O_3-B_2O_3 System: New Compounds and Glass Ceramics Characterisation

Martun Hovhannisyan

Additional information is available at the end of the chapter

http://dx.doi.org/10.5772/52405

1. Introduction

Restriction and an interdiction on use of toxic materials in electronics products since 2006 have promoted an intensification of development new ecologically friendly materials (glasses, glass ceramics, ceramics) with attractive properties. It has stimulated new lead (cadmium) free systems with good glass forming abilities investigations and new stoiciometric and eutectic points revealing and characterization. Alkaline-earth bismuth borate ternary systems were a good candidate for this purpose, because the binary Bi_2O_3-B_2O_3 system have propensity for glass formation and set of binary compounds and eutectics [1 - 3]. Furthermore, bismuth borate single crystals and glass ceramics have nonlinear optical (NLO) properties and other attractive properties [4 - 7]. Both these factors are reasons for further study of binary and ternary bismuth borate systems, and the glasses which they form.

The phase diagram of the Bi_2O_3–B_2O_3 system was first determined by Levin &Daniel in 1962 [2] and five crystalline compounds, $Bi_{24}B_{12}O_{39}$, $Bi_4B_2O_9$, $Bi_3B_5O_{12}$, BiB_3O_6 and $Bi_2B_8O_{15}$, were identified. Later Pottier revealed a sixth compound, $BiBO_3$ (bismuth orthoborate) [8], which was missing in the original phase diagram [2]. There are no doubts about the existence of $BiBO_3$ now: Becker with co-workers have confirmed existence of bismuth orthoborate [5, 9, 10] and its transparent colourless single crystals of $BiBO_3$ have recently been grown from the melt and characterized by Becker & Froehlich [10]. Monophase samples of both crystalline $BiBO_3$ modifications were obtained by crystallisation below 550°C of bismuth borate glasses with 50-57 mol% B_2O_3 [10]. However, these authors did not correct the phase diagram, and did not determine the melting point of $BiBO_3$ or the eutectic composition between $BiBO_3$ and $Bi_3B_5O_{12}$. The compound $BiBO_3$ and this eutectic point are clearly given on the Zargarova & Kasumova's version of the B_2O_3–Bi_2O_3 phase diagram, without indication of their melting points and the eutectic composition [11].

Kargin with co-authors [12] by DTA and X-ray analysis have studied conditions of metastable phases formation at system Bi_2O_3-B_2O_3 melts crystallization. They have confirmed existence of metastable $BiBO_3$ compound and for the first time have specified on congruent character of its melting. Authors also establish formation of a metastable phase of $5Bi_2O_3 \bullet 3B_2O_3$ composition. Both compounds together with initial Bi_2O_3 and B_2O_3 are present on the metastable state diagram of the Bi_2O_3-B_2O_3 system constructed by them.

Presence of five compounds on the known Bi_2O_3-B_2O_3 phase diagram has naturally led to formation of five eutectics compositions containing (mol % B_2O_3): 19.14 (622°C), 44.4 (646 °C), 73.5 (698°C), 76.6 (695°C) and 81.04 (709°C). There is an area of phase separation traditional for borate systems, observed for compositions containing 81-100 mol % B_2O_3 [2]. Though according to [12], the area of stable phase separation is stretched to 58-95 mol % B_2O_3.

Interest to ternary alkali free bismuth borate systems M_xO_y-Bi_2O_3-B_2O_3 (M=Zn,Sr,Ca,Ba) studies has amplified recently. Various research groups (Russian, Canadian, Armenian) worked in this area during 1990-2009 and revealed a number of ternary compounds, determined their structure, optical and nonlinear optical properties. Thus, three ternary zinc bismuth borate compounds have been revealed in the ZnO-Bi_2O_3-B_2O_3 system. At first Zargarova& Kasumova have revealed $ZnBi_4B_2O_{10}$ and $ZnBiBO_4$ compounds [11]. Later Barbier with co-authors by solid-state reaction have synthesized third melilite type $ZnBi_2B_2O_7$ compound with large SHG (four time higher as KDP) [13].

Barbier & Cranswick at first two novel noncentrosymmetric $MBi_2B_2O_7$ or $MBi_2O(BO_3)_2$ (M=Ca, Sr) compounds have synthesized by solid-state reactions in air at temperatures in the 600–700°C range [14]. Their crystal structures have been determined and refined using powder neutron diffraction data. $CaBi_2B_2O_7$ compound has SHG response two time higher as KDP [14]. However, authors didn't pay attention for both compounds melting behavior.

Egorisheva with co-authors have studied phase relation in the CaO-Bi_2O_3-B_2O_3 system and constructs the 600 °C (subsolidus) section of its phase diagram [15]. A new ternary compound of composition $CaBi_2B_4O_{10}$ was identified and the existence of $CaBi_2B_2O_7$ ternary compound was comfirmed. Both compounds had incongruent melting at 700 and 783 °C respectively and liquidus temperature about 900-930 °C.

Kargin with co-workers have studied phase relation in the SrO-Bi_2O_3-B_2O_3 system in subsolidus at 600 °C [16]. Two new ternary compound of $Sr_7Bi_8B_{18}O_{46}$ and $SrBiBO_4$ compositions were identified. Both compounds had incongruent melting at 760 and 820 °C without indication liquidus temperature. However, later Barbier et el. have discribe new novel centrosymmetric borate $SrBi_2OB_4O_9$ ($SrBi_2B_4O_{10}$) forming in the SrO–Bi_2O_3–B_2O_3 system [17], thereby having substituted under doubt existence of previously reported $Sr_7Bi_8B_{18}O_{46}$ compound [16].

The uniqueness of the BaO-Bi_2O_3-B_2O_3 system is shown by the available sets of compounds and eutectics both in the binary Bi_2O_3–B_2O_3 and BaO–B_2O_3 systems. Seven compounds are known in the BaO-B_2O_3 system. Four congruent melting binary compounds $Ba_3B_2O_6$, BaB_2O_4, BaB_4O_7, BaB_8O_{13} with melting points(m.p.) 1383, 1105, 910, 889°C accordingly were found by Levin & McMurdie [18, 19]. Further, Green and Wahler have found out new congruent melted at 890°C $Ba_2B_5O_{17}$ compound at the ternary BaO-B_2O_3-Al_2O_3 system investigation [20].

http://dx.doi.org/10.5772/52405

Hubner confirmed an existence of the congruent melted $Ba_2B_5O_{17}$ compound with m.p. 890 °C, and revealed two new compounds $Ba_4B_2O_7$, $Ba_2B_2O_5$ [21]. However, all scientists and researches have used the melting diagram of the $BaO-B_2O_3$ system created by Levin & McMurdie up to now, without the indication in it the specific areas of existence of new compounds and eutectic points among them [18].

Both these factors were the reason of the $BaO-B_2O_3$ system phase diagram correction made by Hovhannisyan R.M. [22]. Author has revealed fields of $Ba_2B_5O_{17}$ and BaB_4O_7 compounds crystallisation and new eutectic points which are absent on the diagram constructed by Levin & McMurdie [18]. Six binary eutectic compositions containing 31.5, 37.5, 63.5, 68.5, 76.0, 83.4 mol % B_2O_3 with melting points 1025, 915, 905, 895, 869 and 878°C accordingly were on the diagram after correction.

Area of two immiscible liquids established by Levin & McMurdie [35] in the $BaO-B_2O_3$ in an interval of 1.5 to 30wt. % BaO content, it has been confirmed in the subsequent by other authors. However, the temperature of the liquation couple, which are 1150, 1180, 1256 °C according to [23] and 1539°C according to [24] is discussed till now.

There are no full version of the phase diagram of the $BaO-Bi_2O_3$ system till now [1]. It is very complex system, which is very critical to atmosphere and pressure at experiment carrying out [25 - 28]. Two low melted eutectic areas (740-790°C) clear observed on phase diagram studied in air or oxigen in high bismuth content region around 5-7 mol%BaO and 25-30 mol %BaO [26 - 28].

All research groups payd special attention to $BaO-Bi_2O_3-B_2O_3$ system studies and new ternary compounds revealing and characterisation. Barbier *et al.* have studied seven compositions in the ternary $BaO-B_2O_3-Bi_2O_3$ system by solid state synthesis at temperatures below 650°C and $BaBiBO_4$, or $BaBi(BO_3)O$, a novel borate compound, has been made and chracterisised [29]. Above 650°C it decays with bismuth borate glass formation. A powder sample of $BaBiBO_4$ had a second harmonic signal with a NLO efficiency equal to five times that of KDP.

Practically in parallel, Egorysheva with co-workers have been investigated phase equilibrium in the $Bi_2O_3-BaB_2O_4-B_2O_3$ system by X-ray analysis and DTA [30, 31]. Studies were spent by the samples solid state synthesis in closed Pt crucibles in muffle furnaces at the temperature range 500-750 ^{0}C, that corresponds to sub-solidus area. The synthesis duration (with intermediate cakes regrinding) were 6-16 days. They confirmed presence of $BaBiBO_4$ and have revealed three new compounds: $BaBiB_{11}O_{19}$, $BaBi_2B_4O_{10}$, $Ba_3BiB_3O_9$. $BaBiB_{11}O_{19}$, $BaBi_2B_4O_{10}$ have congruent melting at 830 and 730 °C respectively and $BaBiBO_4$ melt incongruently at 780^{0}C. $Ba_3BiB_3O_9$ undergoes a phase transition at 850°C and exist up to 885°C, were decompose in the solid state [31].

Recently single crystals of $BaBi_2B_4O_{10}$ composition were grown by cooling of a melt with the stoichiometric composition with cooling rate 0.5 K/h [32]. They have once again confirmed existence of $BaBi_2B_4O_{10}$ stoichometric compound earlier obtained by solid state synthesis.

In 1972 Elwell with co-workers investigated the $BaO–B_2O_3–Bi_2O_3$ system by hot stage microscopy and a new ternary eutectic composition, $23.4BaO•62.4Bi_2O_3•14.2B_2O_3$ (wt%), with a low liquidus temperature of 600°C, was revealed for ferrite spinel growth [33].

Using different melts cooling rates Hovhannisyan, M. with co-authors at first have determined large glass-forming field in the $BaO-Bi_2O_3-B_2O_3$ system, which includes all eutectics in the binary $Bi_2O_3-B_2O_3$, $BaO-B_2O_3$ and $BaO-Bi_2O_3$ systems and covers majority of the concentration triangles, reaching up to 90 mol% Bi_2O_3. [34, 35].

The methodology based on glass samples investigation was more effective at $BaO-Bi_2O_3-B_2O_3$ system phase diagram construction, than a traditional technique based on solid state sintered samples studies. Because DTA curves of glasses, to the contrary DTA curves of solid state sintered samples, indicates their all characteristics temperatures, includes exothermal effects of glass crystallizations and endothermic effects of formed crystalline phases melting. It has allowed us to reveal two new $BaBi_2B_2O_7$ and $BaBi_{10}B_6O_{25}$ congruent melted at 725 and 690°C respectively compounds in the $BaO-Bi_2O_3-B_2O_3$ system [34 - 36].

However, our further studies of glasses and glass ceramics in this system have shown necessity of glass forming diagram correction and phase diagram construction in the ternary $BaO-Bi_2O_3-B_2O_3$ system and present these data to scientific communitty. Another aim of this work is both known and novel stoichiometric ternary barium bismuth borates compounds characterisation in glassy, glass ceramic and ceramic states for further practical application.

2. Experimental

About three hundred samples of various binary and ternary compositions have been synthesized and tested in $BaO- Bi_2O_3-B_2O_3$ system. Compositions were prepared from "chemically pure" grade $BaCO_3$, H_3BO_3 and Bi_2O_3 at 2.5-5.0 mol % intervals. The most part of samples has been obtained as glasses by various cooling rates depending on melts glass forming abilities: as bulk glass plates with thickness 6,5 ÷7mm by casting on metallic plate (up to 10^{K}/s), as monolithic glass plates with thickness up to 3mm by casting between two steel plates(~10^{2} ^{K}/s), and glass tapes samples with thickness 30–400 μm through super cooling method (10^{3}÷10^{4} ^{K}/s). Glass formation was determined visually or by x-ray analysis. The glass melting was performed at 800–1200°C for 15–20 min with a 20–50 g batch in a 20–50 ml uncovered quartz glass or corundum crucible, using an air atmosphere and a "Superterm 17/08" electric furnace. Compositions in the $BaO-B_2O_3$ system were melted in a 25 or 50 ml uncovered Pt crucibles at 1400–1500°C for 30 min with a 20–50 g batch. The chemical composition of some glasses was determined by traditional chemical analysis, and the results indicate a good compatibility between the calculated and analytical amounts of B_2O_3, BaO and Bi_2O_3. SiO_2 contamination from quartz glass crucibles did not exceed 2 wt%, and alumina contamination did not exceed 0 5–1 wt%, according to the chemical analysis data.

Samples of compositions laying outside of a glass formation field or having high melting temperature, have been obtained by solid-phase synthesis. Mixes (15-20 g) were carefully

http://dx.doi.org/10.5772/52405

frayed in an agate mortar, pressed as tablets, located on platinum plates and passed the thermal treatment in "Naber"firm electric muffles. After regrinding powders were tested by DTA and X-ray methods. The synthesized samples of binary barium borate system compositions containing 60 mol% and more of BaO and also compositions containing over 90mol % B_2O_3 had very low chemical resistance and were hydrolyzed on air at room temperature. In this connection the synthesized samples were kept in a dryer at 200°C.

DTA and X-ray diffraction data of glass and crystallized glass samples have been used for phase diagram construction in the ternary BaO- Bi_2O_3 -B_2O_3 system. The DTA analysis (pure Al_2O_3 crucible, powder samples weight ~600 mg, heating rates 10 K/min) on Q-1500 type derivatograph were carried out. Glass transition -T_g, crystallization peaks -T_{cr}, melting -T_m and liquidus -T_L temperatures have been determined from DTA curves. Reproducibility of temperatures effects on DTA curves from melting to melting was ±10K. The accuracy of temperature measurement is ±5 K.

Thermal expansion coefficient (TEC) and glass transition temperature (T_g) measurements were made on a DKV-4A type vertical quartz dilatometer with a heating rate of 3K/min. Glass samples in the size of 4×4×50 millimeters have been prepared for TEC measurement. The dilatometer was graduated by the quartz glass and sapphire standards. The TEC measurement accuracy is $\pm(3\div4)\bullet10^{-7}K^{-1}$, T_g ±5 °C.

X-ray patterns were obtained on a DRON-3 type diffractometer (powder method, CuKα–radiation, Ni-filter). Samples for glass crystallization were prepared with glass powder pressed in the form of tablets. Crystallization process was done in the electrical muffles of "Naber" firm by a single-stage heat treatment. This was done within 6-12 hours around a temperature at which the maximum exothermal effects on glasses by DTA were observed.

Crystalline phases of binary and ternary compounds formed both at glasses crystallization and at solid-phase synthesis have been identified by using JCPDS-ICDD PDF-2 release 2008 database [43].

Computerized methodic of ferroelectric hysteresis test and measurement of ferroelectric properties such as coercive field and remanent polarization at wide temperature (up to 250°C and frequency (10-5000Hz) ranges was used. Methodic based on the well known Sawyer – Tower's [44] modified scheme, which is allowing to compensate phase shifts concerned with dielectric losses and conductivity. The desired frequency signal from waveform generator is amplifying by high voltage amplifier and applying to sample. The signals, from the measuring circuit output, proportional to applied field and spontaneous polarization are passing throw high impedance conditioning amplifiers, converting by ADC and operating and analyzing in PC. The technique allows to perform tests of synthesized glass ceramics obtained by means of controlling crystallization of thin (above 30 micrometer thick) monolithic tape (film) specimens by applying up to 300kV/cm field to our thin samples (~50 micrometer thick) and obtain hysteresis loops for wide diversity of hard FE materials.

3. Results

3.1. Glass forming and phase diagrams of the $BaO-Bi_2O_3-B_2O_3$ system

The traditional method of phase diagram construction based on solid-phase sintered samples investigation takes long time and is not effective. The glass samples investigation technique is progressive, because the DTA curves have registered all processes taking place in glass samples, including the processes of glass crystallizations, quantity of crystal phases and temperature intervals of their formation and melting. However, inadequate amount of glass samples restrict their use during phase diagram construction. The super-cooling method promotes the mentioned problem solving and open new possibilities for phase diagrams constructions.

Hovhannisyan R.M. with co-workes successfully developed this direction last time and have constructed phase diagrams in binary and ternary alkiline-eath bismuth borate, barium boron titanate, barium aluminum boron titanate, barium gallium borate, yttrium aluminum borate, yttrium gallium borate, lantanum gallium borate, zinc tellurium molibdate and other systems [34 - 42].

3.1.1. Glass forming diagram of the $BaO-Bi_2O_3-B_2O_3$ system

Figure 1 shows the experimental data on glass formation in the $BaO-Bi_2O_3-B_2O_3$ system obtained by different authors from 1958 to 2007 [45 - 49]. For defining the glass forming ability of the pointed system, the authors of the mentioned works used different amounts of melt, glass melting crucibles, temperature–time melting regimes, and technological methods of melt cooling. Imaoka & Yamazaki studied glass formation by melts cooling on air Glasses were melted at temperatures below 1200 °C in gold-palladium or platinum-rhodium crucibles (Fig.1.1) [45]. Janakirama-Rao glass formation studied by melts cooling on air. Glasses melted in platinum crucibles at 600- 1400 °C with 0.5-1.0 h melts exposition and its cooling in air (Fig. 1.2) [46]. Izumitani [47] experiments spent in 10g crucibles at 1100-1350 °C with melts cooling on air (Fig. 1.3). Milyukov with co-authors glass formation studied by melts casting in steel mold. Glasses melted in platinum crucibles at 600-1400 °C with melts stirring by Pt stirrer for 1h (Fig. 1.4) [48]. Kawanaka & Matusita glass formation studied by silica rod stirred melts pouring into preheated to 250-300°C carbon mold (Fig. 1.5) [49].

Authors used different weights of glass forming melts, melting crucibles, temperature-time of melting regimes and technological methods of melts cooling. Obtained data are difficultly comparable and remote from two basic criteria promoting glass formation: liquidus temperature and speeds of melts cooling.

http://dx.doi.org/10.5772/52405

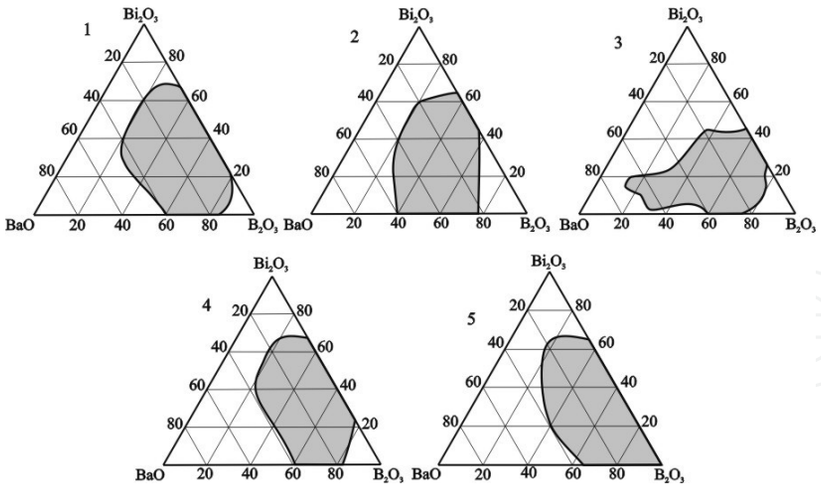

Figure 1. Glass forming regions in the BaO-Bi_2O_3-B_2O_3 system according to the data of the authors: 1- [45], 2-[46], 3-[47], 4-[48], 5-[49].

Figure 2 shows corrected glass formation diagram in the BaO-Bi_2O_3-B_2O_3 system based on phase diagrams of the BaO–B_2O_3, BaO–Bi_2O_3, and B_2O_3–Bi_2O_3 binary systems and controllable melt cooling rates. Using the term "diagram," but not the glass formation region, we take into account the interrelation between the phase diagram and the glass forming ability of the system.

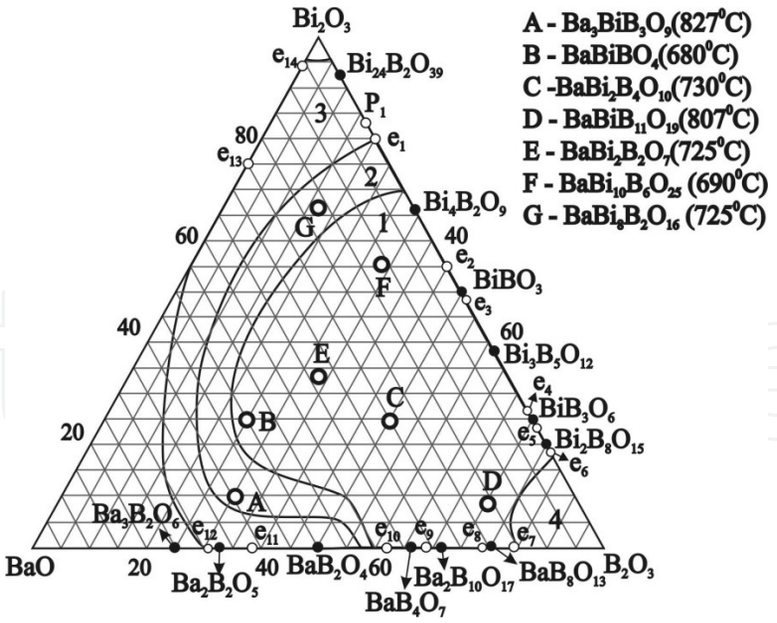

Figure 2. Glass forming diagram in the BaO-Bi_2O_3-B_2O_3 system depending of melts cooling rates: 1-up to 10 K/s; 2~10^2K/s; 3-(10^3-10^4) K/s; 4- stable phase separation region.

Area of glass compositions with low crystallization ability and stable glass formation in the studied ternary BaO-Bi_2O_3 -B_2O_3 system have been determined at melts cooling rate ~ 10 K/s

(Fig.2-1). It included binary $Bi_4B_2O_9$, $BiBO_3$, $Bi_3B_5O_{12}$, BiB_3O_6, $Bi_2B_8O_{15}$, $Ba_2B_{10}O_{17}$, BaB_8O_{13} compounds in the $BaO\text{-}Bi_2O_3$ and $BaO\text{-}B_2O_3$ systems and five ternary $BaBiB_{11}O_{19}$(D), $BaBi_2B_4O_{10}$(C), $BaBi_2B_2O_7$ (E), $BaBi_{10}B_6O_{25}$ (F), and $BaBiBO_4$ (B) compounds. However, we didn't comfirm presence of $Ba_3BiB_3O_9$ (A) compound in area of stable glasses at melts cooling rate ~ 10 K/s, which was reported earlier [34, 35].

Increasing of melts cooling speed up to ~10^2 K/s has led to glass formation area expansion (Fig.2-2). This cooling rate is enough for monolithic glass plates with thickness up to 3mm fabrication by melts casting between two steel plates (Fig.2-2). The glass plates of compositions correspondings to $Ba_3BiB_3O_9$ (A) and supposed $BaBi_8B_2O_{16}$ (G) compounds have been obtained by this way.

Super cooling technique constructed by our group allowed to expand the borders of glass formation in studied system under high melts cooling rates equal to (10^3-10^4) K/s (Fig.2-3). Determined glassforming area include compositions content: 80 – 95 mol% Bi_2O_3 in the binary B_2O_3–Bi_2O_3 system; 43-70 mol% BaO in the binary BaO–B_2O_3 system, including BaB_2O_4 composition. Area of glass formation from both these areas moves to 55-95 mol% content compositions in the binary BaO–Bi_2O_3 system (Fig.2-3).

Traditional for borate systems a stable phase separation region was also observed for high B_2O_3 content compositions contents more than 84 -87 mol%B_2O_3 (Fig.2-4).

3.1.2. Phase diagram of the BaO-Bi_2O_3-B_2O_3 system

Our investigation of the ternary $BaO\text{-}B_2O_3\text{-}Bi_2O_3$ system have purposefully been directed on construction of the phase diagram through first of all glass forming diagram construction and revealing both new compounds and eutectic compositions. Constructed by us glass forming diagram (Fig.2) practically occupies the most part of the $BaO\text{-}B_2O_3\text{-}Bi_2O_3$ concentration triangles. It has allowed to use synthesized glasses as initial compositions at phase diagram construction. It was basic difference of our methodology from technologies used by other authors. Phase equilibriums reached at isothermal sections construction do not allow to have a full picture of processes in cases of the solid state synthesized samples investigations. Whereas at glass samples studies we determine not only characteristic points of glasses(T_g and T_s) by DTA, but also quantity of crystal phases, temperatures of their crystallization and then temperatures of their melting. It has allowed us to reveal new stoichiometric compositions which have been lost by other research groups at isothermal sections construction by traditional methods. In some cases we also in parallel used samples obtained by solid state synthesis for comparison with their glassy analogues or in those cases, when their obtaining in the glassy form was impossible.

http://dx.doi.org/10.5772/52405

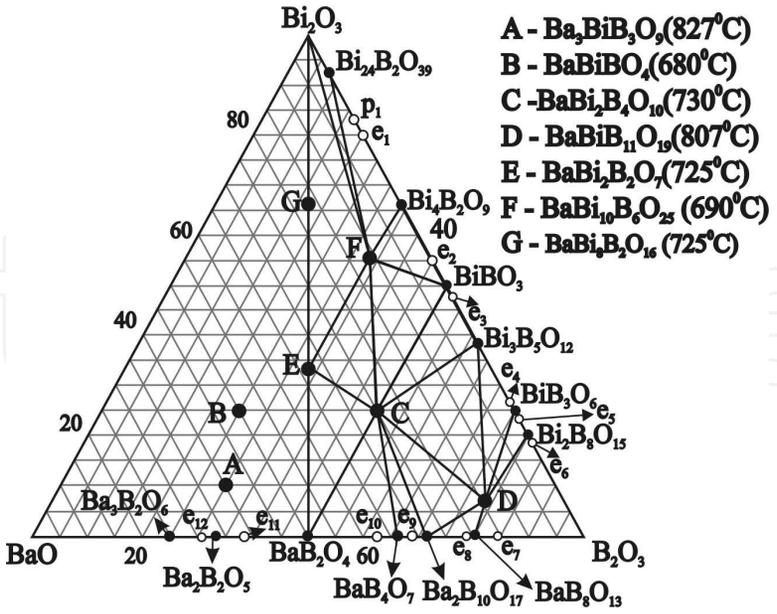

Figure 3. The BaO-B_2O_3-Bi_2O_3 system triangulation

Experimental data concerning phase diagrams of binary systems Bi_2O_3-B_2O_3, BaO-B_2O_3, BaO-Bi_2O_3 and pseudo-binary sections in the BaO-B_2O_3-Bi_2O_3 system have allowed us to estimate fields of primary crystallization of co-existing phases and divided all concentration triangle into elementary triangles, i.e. to make triangulation.

The triangulation scheme in the BaO-B_2O_3-Bi_2O_3 system is presented on Fig. 3. By means of a triangulation all concentration triangle is divided into following elementary triangles: $BiBO_3$-F-C, $BiBO_3$-F-$Bi_4B_2O_9$, $BiBO_3$-C-$Bi_3B_5O_{12}$, F-E-C, C-BaB_2O_4-E, C-$Bi_3B_5O_{12}$-D, $Bi_4B_2O_9$-F-Bi_2O_3, E-Bi_2O_3-F, C-BaB_2O_4-$Ba_2B_{10}O_{17}$, $Ba_2B_{10}O_{17}$-D-C, $Ba_2B_{10}O_{17}$-D-B_2O_3, $Bi_3B_5O_{12}$-D-$Bi_2B_8O_{15}$, D-$Bi_2B_8O_{15}$-B_2O_3.

3.1.2.1. Phase diagram of the binary Bi_2O_3–B_2O_3 system

First of all we have attempt to finished phase diagram construction in area of compositions around of $BiBO_3$ compound. Compositions containing 45–65 mol% B_2O_3 in the Bi_2O_3–B_2O_3 system were tested to determine the melting point of $BiBO_3$ and to determine the eutectic composition between $BiBO_3$ and $Bi_3B_5O_{12}$. The compositions used to correct the B_2O_3–Bi_2O_3 phase diagram were prepared by solid state synthesis at 520°C, with steps of 0.5–1.0 mol% B_2O_3 over the interval 45–55 mol% B_2O_3. As a result, the eutectic composition, 48.5Bi2O3•51.5B2O3 (mol%), between $BiBO_3$ and $Bi_3B_5O_{12}$, was determined, and its melting point was measured by DTA as 665±5°C (Fig. 4). It was also found that $BiBO_3$ melts congruently at 685±5°C.

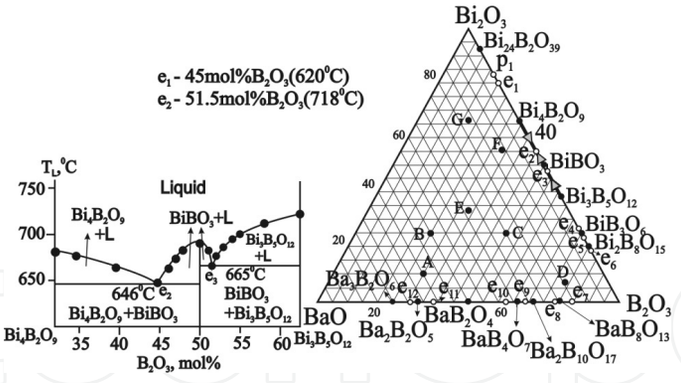

Figure 4. Corrected phase diagram of the Bi_2O_3-B_2O_3 system in the interval 30–65 mol% B_2O_3.

3.1.2.2. Phase diagram of the pseudo-binary $BiBO_3$–BaB_2O_4 system

$BaBi_2B_4O_{10}$ is a congruently melting compound, with a melting point of 730°C, and it occupies the central area of the $BiBO_3$–BaB_2O_4 pseudo-binary system (Fig. 5). This system forms two simple pseudo-binary eutectics, E_1 at 15 mol% BaB_2O_4, with a melting point of 620°C, and E_2 at 60 mol% BaB_2O_4, with a melting point of 718°C.

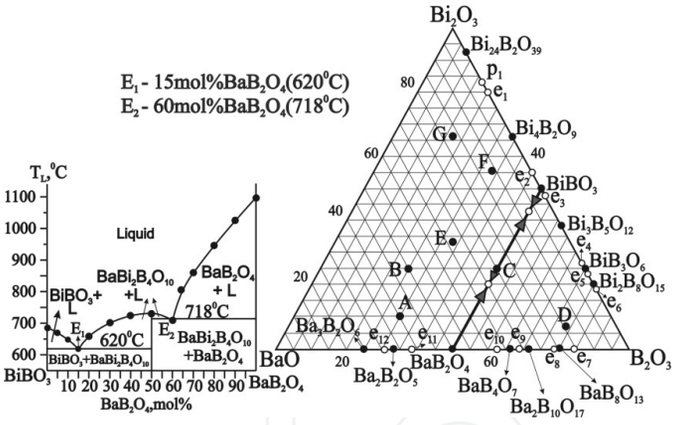

Figure 5. Phase diagram of the pseudo-binary system $BiBO_3$-BaB_2O_4

3.1.2.3. Phase diagram of the pseudo-binary $Bi_4B_2O_9$–$BaBi_2B_2O_7$ system

The introduction of 12 mol% $BaBi_2B_2O_7$ in the pseudo-binary system $Bi_4B_2O_9$-$BaBi_2B_2O_7$ reduced the melting point of initial $Bi_4B_2O_9$, and resulted in the formation of a simple pseudo-binary eutectic, E_3, with melting point 605°C (Fig. 6). A maximum of the liquidus with melting point of 690°C is seen at 33.33 mol% $BaBi_2B_2O_7$, which indicates the formation of the new congruently melting ternary compound $BaBi_{10}B_6O_{25}$ ($11.11BaO \bullet 55.55Bi_2O_3 \bullet 33.33B_2O_3$). Further increase of the $BaBi_2B_2O_7$ content (49 mol%) leads to a second pseudo-binary eutectic, E_4, with melting point 660°C. Increasing of the liquidus temperature is observed in the post eutectic region of composition, with a maximum at 725°C. It corresponds to the formation of the new congruently melting ternary compound $BaBi_2B_2O_7$ (Fig. 6).

http://dx.doi.org/10.5772/52405

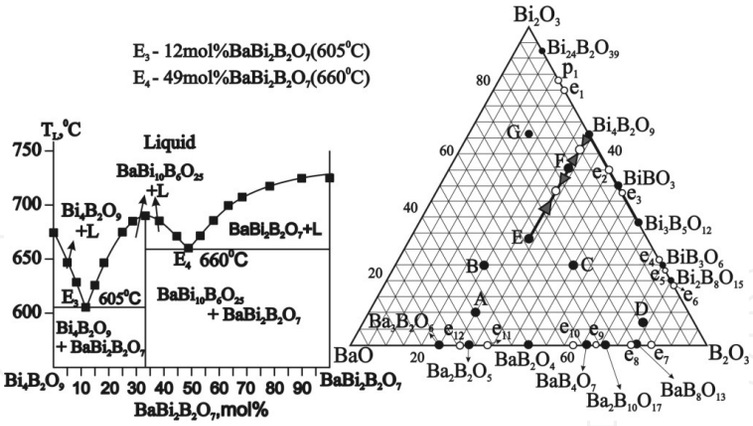

Figure 6. Phase diagram of the pseudo-binary system $Bi_4B_2O_9$-$BaBi_2B_2O_7$.

Two new crystalline ternary compounds, $BaBi_2B_2O_7$ and $BaBi_{10}B_6O_{25}$, were revealed by crystallisation at the same glass composition. Both compounds, $BaBi_2B_2O_7$ and $BaBi_{10}B_6O_{25}$, melt congruently at 725±5°C and 690±5°C, respectively. The X-ray characteristics of $BaBi_2B_2O_7$ and $BaBi_{10}B_6O_{25}$ were determined and are given in Tables 1 and 2.

No.	d_{exp}	I/I_0	hkl	No.	d_{exp}	I/I_0	hkl	No.	d_{exp}	I/I_0	hkl
1	6.23	9	101	20	2.15	25	140	39	1.349	7	125
2	5.02	9	111	21	2.12	5	232	40	1.33	3	543
3	4.80	5	201	22	2.06	24	123	41	1.28	8	035
4	4.29	5	020	23	2.01	6	523	42	1.24	6	560
5	4.11	14	120	24	1.977	25	241	43	1.217	5	263
6	3.88	6	300	25	1.84	15	142	44	1.21	9	843
7	3.67	4	021	26	1.826	7	133	45	1.206	13	271
8	3.59	26	301	27	1.786	6	004	46	1.19	14	145
9	3.56	50	121	28	1.729	52	114	47	1.173	12	245
10	3.52	23	220	29	1.679	23	250	48	1.17	4	1010
11	3.19	100	112	30	1.636	34	251	49	1.14	6	126
12	3.12	8	221	31	1.63	5	532	50	1.11	6	662
13	3.05	9	202	32	1.57	4	052	51	1.10	6	326
14	2.91	43	030	33	1.556	10	243	52	1.09	4	180
15	2.696	90	122	34	1.522	8	034	53	1.042	6	146
16	2.51	12	222	35	1.488	23	632	54	1.021	9	065
17	2.376	21	003	36	1.458	6	060	55	1.018	9	943
18	2.31	5	421	37	1.428	10	811	56	1.01	5	274
19	2.254	22	113	38	1.373	11	821				

Table 1. X-ray characteristics of the new ternary compound $BaBi_2B_2O_7$, synthesized at the same glass composition crystallization (640°C, 20 h).

Single crystals of $BaBi_{10}B_6O_{25}$ were obtained by cooling of a melt with the stoichiometric composition. Glass powder of composition $11.11BaO•55.55Bi_2O_3•33.33B_2O_3$ (mol%) was heated in a quartz glass ampoule up to 750°C at a rate 10 K/min. After 2 h exposition at high temperature, the melt was cooled at a rate 0.5 K/h. Single crystals with sizes up to 1.66×0.38×0.19 mm^3 were grown.

No.	d_{exp}	I/I_0	hkl	No.	d_{exp}	I/I_0	hkl	No.	d_{exp}	I/I_0	hkl
1	9.21	3.0	012	23	2.91	31	0110	45	2.01	5.2	321
2	6.26	3.0	101	24	2.8	6	221	46	1.98	23.7	323
3	6.02	3.0	005	25	2.7	75.9	206	47	1.92	3.0	1214
4	5.01	7.3	006	26	2.64	3.4	045	48	1.88	3.0	0314
5	4.89	10.8	104	27	2.57	3.0	2.07	49	1.86	3.0	162
6	4.63	6.5	024	28	2.53	4.3	046	50	1.84	15.1	254
7	4.19	4.3	025	29	2.52	5.2	144	51	1.83	3.0	1412
8	4.18	4.3	122	30	2.49	6.9	230	52	1.82	3.0	164
9	4.11	10	115	31	2.47	9.5	1210	53	1.81	3.0	255
10	3.92	6.0	030	32	2.45	4.7	232	54	1.79	3.4	165
11	3.80	3.4	032	33	2.38	16	0310	55	1.77	3.0	328
12	3.65	10.8	033	34	2.35	4.3	050	56	1.75	3.4	1413
13	3.56	39.7	107	35	2.34	5.2	051	57	1.73	55.2	341
14	3.51	9.5	125	36	2.33	3.9	1012	58	1.71	4.3	343
15	3.41	3.4	117	37	2.31	3.4	1212	59	1.69	3.0	069
16	3.38	7.3	130	38	2.25	17.2	228	60	1.68	16.4	070
17	3.33	8.6	131	39	2.21	7.8	150	61	1.65	3.0	259
18	3.27	9.1	132	40	2.19	3.0	055	62	1.64	31.0	074
19	3.18	100	133	41	2.15	21.2	237	63	1.61	2.9	400
20	3.07	14.7	203	42	2.09	3.4	312	64	1.6	6.0	402
21	3.04	9.2	212	43	2.06	21.6	304	65	1.55	6.5	421
22	2.94	14.2	040	44	2.03	3.0	314	66	1.52	9.5	177

Table 2. X-ray characteristics of the new ternary $BaBi_{10}B_6O_{25}$ single crystals.

The x-ray powder diffraction patterns of $BaBi_2B_2O_7$ and $BaBi_{10}B_6O_{25}$ could be indexed on an orthorhombic cell with lattice parameters as follows:

- for $BaBi_2B_2O_7$ a=11.818 Å, b=8.753 Å, c=7.146 Å, cell volume V=739.203 $Å^3$, Z=4;
- for $BaBi_{10}B_6O_{25}$ a=6.434 Å, b=11.763 Å, c=29.998 Å, cell volume V=2270.34 $Å^3$, Z=8.

3.1.2.4. Phase diagram of the pseudo-binary $BiBO_3$–$BaBi_{10}B_6O_{25}$ system

$BiBO_3$– $BaBi_{10}B_6O_{25}$ is a very important system (Fig.7). Initial $BiBO_3$ has a melting point of 685°C. The second maximum in the liquidus curve (Fig.7) of 690°C is connected with the for-

http://dx.doi.org/10.5772/52405

mation of the new ternary compound $BaBi_{10}B_6O_{25}$. There is a simple pseudo-binary eutectic E_5 between these two compounds at 54 mol%$BaBi_{10}B_6O_{25}$, with a melting point of 595°C.

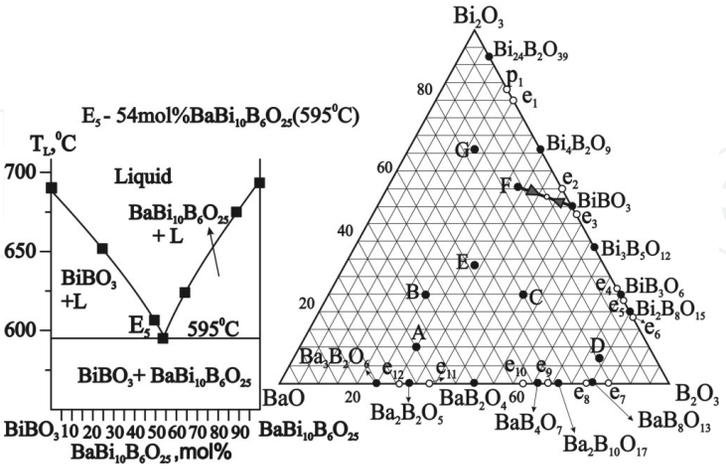

Figure 7. Phase diagram of the pseudo-binary system $BiBO_3$- $BaBi_{10}B_6O_{25}$.

3.1.2.5. Phase diagram of the pseudo-binary $BaBi_{10}B_6O_{25}$ - $BaBi_2B_4O_{10}$ system

The $BaBi_{10}B_6O_{25}$–$BaBi_2B_4O_{10}$ system confirms the presence of the new congruently melting ternary compound $BaBi_{10}B_6O_{25}$, with a melting point of 690°C (Fig.8). $BaBi_2B_4O_{10}$ melts congruently at 730°C. There is a simple pseudo-binary eutectic E_6 between these two compounds at 28 mol % $BaBi_2B_4O_{10,}$ with a melting point of 660°C.

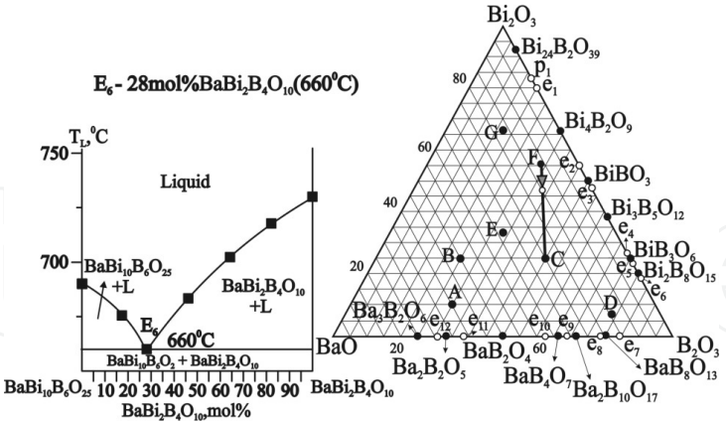

Figure 8. Phase diagrams of the pseudo-binary system $BaBi_{10}B_6O_{25}$ -$BaBi_2B_4O_{10}$.

3.1.2.6. Phase diagram of the pseudo-binary $BaBi_2B_4O_{10}$ – 50BaO•50Bi_2O_3 section

This pseudo-binary section consists of two ternary compounds $BaBi_2B_4O_{10}$, $BaBi_2B_2O_7$ and two eutectics E_7, E_8 dividing fields primary crystallisations these compounds. Initial composition is $BaBi_2B_4O_{10}$ (Fig.9). The introduction of 20 mol% 50%BaO•50%Bi_2O_3 in the pseudo-binary

system $BaBi_2B_4O_{10}$ – 50BaO•50Bi_2O_3 reduced the melting point of initial $BaBi_2B_4O_{10}$, and resulted in the formation of a simple pseudo-binary eutectic, E_7, with melting point 680°C (Fig.9). A maximum of the liquidus with melting point of 725°C is seen at 33.33 mol% of 50%BaO•50%Bi_2O_3, which indicates the formation of the new congruently melting ternary compound $BaBi_2B_2O_7$. Further increase of the 50%BaO•50%Bi_2O_3 content (52.5 mol%) leads to a second pseudo-binary eutectic, E_8, with melting point 700°C. Increasing of the liquidus temperature is observed in the post eutectic region of composition (more than 52.5mol% of 50BaO•50Bi_2O_3). Un identified phase is in the post eutectic (E_8) region of composition (Fig.9).

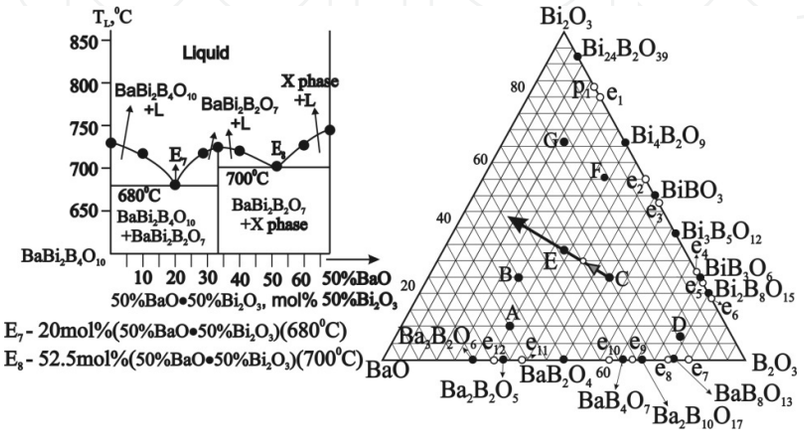

Figure 9. Phase diagram of the pseudo-binary section $BaBi_2B_4O_{10}$ – 50BaO•50Bi_2O_3.

3.1.2.7. Phase diagram of the pseudo-binary BaB_2O_4–Bi_2O_3 section

BaB_2O_4 - Bi_2O_3 section consist of two pseudo-binary BaB_2O_4- $BaBi_2B_2O_7$, $BaBi_2B_2O_7$- Bi_2O_3 systems (Fig.10). There are two eutectics: E_9 between BaB_2O_4 and $BaBi_2B_2O_7$, E_{10} between $BaBi_2B_2O_7$ and $BaBi_8B_2O_{16}$, and peritectic point P_1 between $BaBi_8B_2O_{16}$ and Bi_2O_3 (Fig.10). The introduction of 26 mol% Bi_2O_3 in the pseudo-binary system BaB_2O_4 – Bi_2O_3 sharp reduced the melting point of initial BaB_2O_4 on 445^{0}C, and resulted in the formation of a simple eutectic, E_9, with melting point 685°C (Fig.10). A maximum of the liquidus with melting point of 725°C is seen at 33 33 mol% of Bi_2O_3, which indicates the formation of the new congruently melting ternary compound $BaBi_2B_2O_7$.

Further increase of the Bi_2O_3 content (42 mol%) leads to a second eutectic, E_{10}, formation with melting point 690°C. Increasing of the liquidus temperature is observed in the post eutectic region of composition (more than 42mol% of Bi_2O_3) and formation of new incongruent melted at 725 °C $BaBi_8B_2O_{16}$ ternary compound (Fig.10). It is very difficult determined of $BaBi_8B_2O_{16}$ X-ray characteristics, because they very closed to Bi_2O_3 characteristics.

Constructed by us this section's diagram essentially differs from that constructed by Russian researches Egorisheva & Kargin [30] because they could not find out two new compounds revealed by us: congruent melted at 725°C $BaBi_2B_2O_7$ and incongruent melted at 725°C $BaBi_8B_2O_{16}$(Fig.10). At repeated, even more detailed studies they also could not find out these compounds [31].

http://dx.doi.org/10.5772/52405

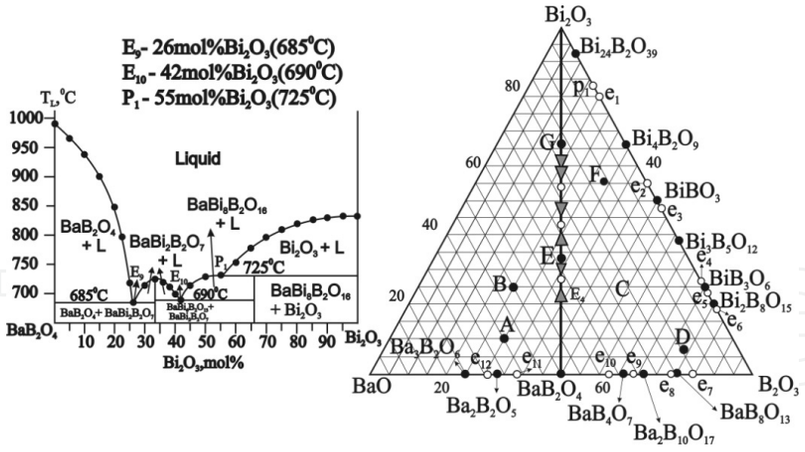

Figure 10. Phase diagram of the BaB_2O_4 – Bi_2O_3 section.

3.1.2.8. Phase diagram of the pseudo-binary $Bi_3B_5O_{12}$ – $BaBi_2B_4O_{10}$ system

It is very simple system with pseudo-binary eutectic E_{11} between two congruent melted $Bi_3B_5O_{12}$ and $BaBi_2B_4O_{10}$ compounds. Eutectic E_{11} content 38 mol% of $BaBi_2B_4O_{10}$ and has melting point 680°C (Fig.11).

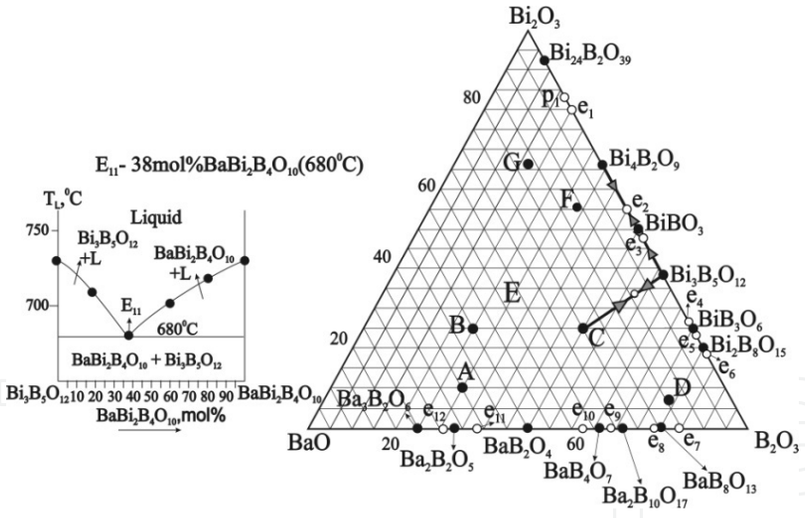

Figure 11. Phase diagram of the pseudo-binary system $Bi_3B_5O_{12}$ – $BaBi_2B_4O_{10}$

3.1.2.9. Phase diagram of the pseudo-binary $BaBi_2B_4O_{10}$ – $BaBiB_{11}O_{19}$ system

Initial $BaBi_2B_4O_{10}$ has a melting point of 730°C. The second maximum in the liquidus curve (Fig.12) of 807°C is connected with the formation of the ternary compound $BaBiB_{11}O_{19}$. There is a simple pseudo-binary eutectic, E_{12}, between these two compounds at 65.5 mol% Ba-$Bi_2B_4O_{10}$, with a melting point of 695°C.

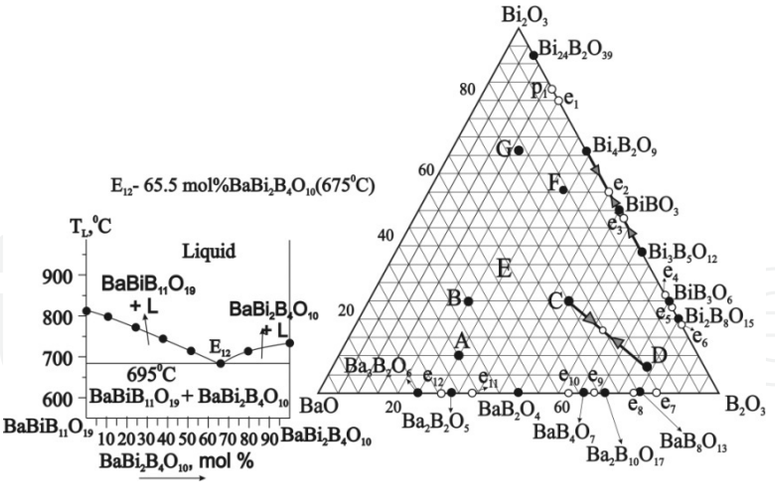

Figure 12. Phase diagram of the pseudo-binary system $BaBi_2B_4O_{10} – BaBiB_{11}O_{19}$.

3.1.2.10. Phase diagram of the pseudo-binary $Bi_3B_5O_{12} – BaBiB_{11}O_{19}$ system

Pseudo-binary system $Bi_3B_5O_{12}$ -$BaBiB_{11}O_{19}$ has simple eutectic E_{13} formed between two congruent melted $BaBiB_{11}O_{19}$ and $Bi_3B_5O_{12}$ compounds. According to DTA eutectic E_{13} has melting point 705°C and content 28 mol% $BaBiB_{11}O_{19}$ (Fig.13).

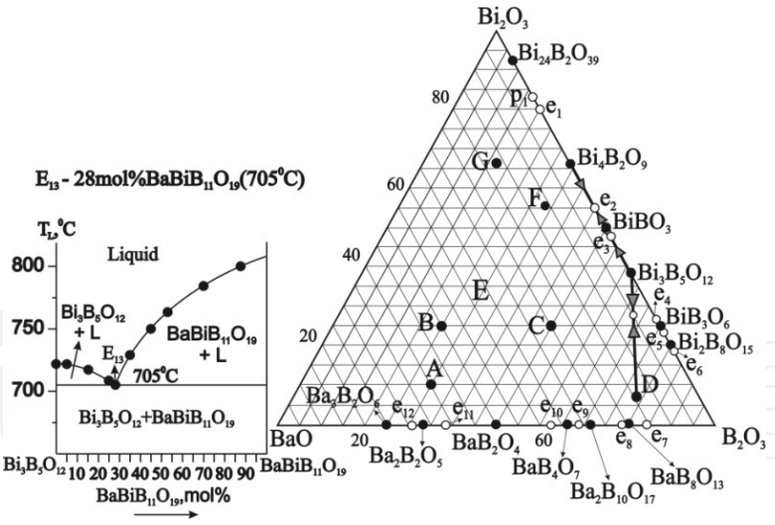

Figure 13. Phase diagram of the pseudo-binary system $Bi_3B_5O_{12}$ - $BaBiB_{11}O_{19}$.

3.1.2.11. Phase diagram of the pseudo-binary $BaBiB_{11}O_{19} – Ba_2B_{10}O_{17}$ system

Pseudo-binary system $BaBiB_{11}O_{19} – Ba_2B_{10}O_{17}$ has simple eutectic E_{14} formed between two congruent melted compounds $Ba_2B_{10}O_{17}$ and $BaBiB_{11}O_{19}$. According to DTA eutectic E_{14} has melting point 780°C and content 26 mol% $Ba_2B_{10}O_{17}$(Fig.14).

http://dx.doi.org/10.5772/52405

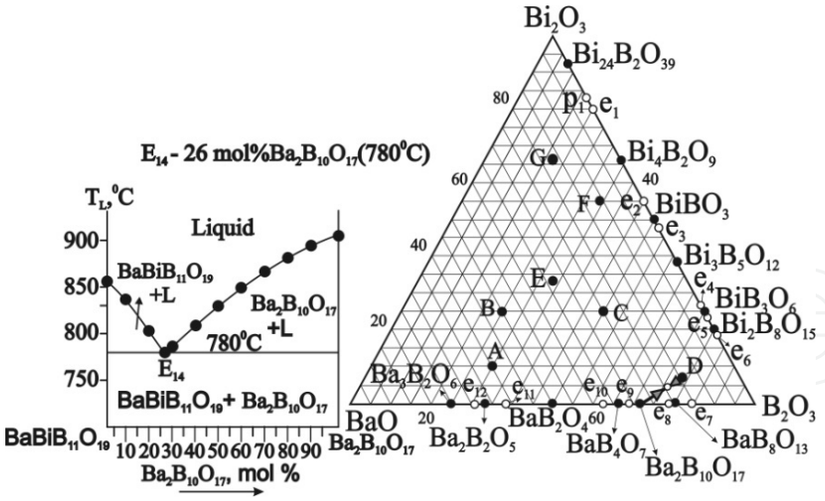

Figure 14. Phase diagram of the pseudo-binary system $BaBiB_{11}O_{19}$ – $Ba_2B_{10}O_{17}$.

3.1.2.12. Phase diagram of the pseudo-binary $BaBi_2B_4O_{10}$ – $Ba_2B_{10}O_{17}$ system

It is very simple system with eutectic E_{15} formed between two congruent melted $Ba_2B_{10}O_{17}$ and $BaBi_2B_4O_{10}$ compounds. Pseudo-binary eutectic E_{15} content 24 mol% of $Ba_2B_{10}O_{17}$ and has melting point 710°C (Fig. 15).

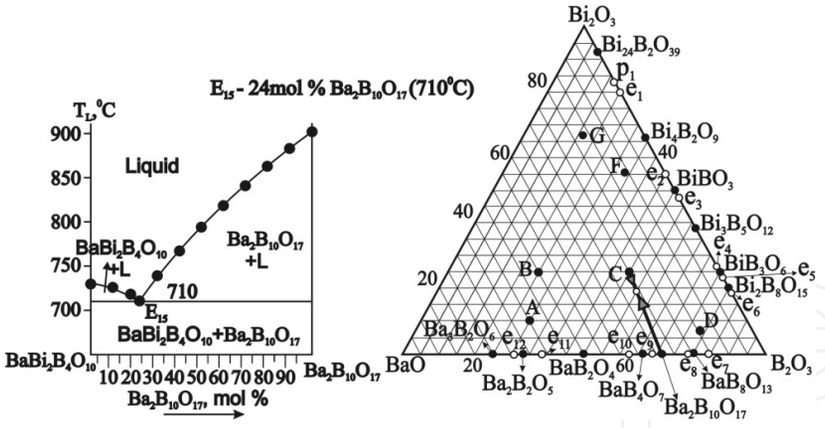

Figure 15. Phase diagram of the pseudo-binary system $BaBi_2B_4O_{10}$ – $Ba_2B_{10}O_{17}$.

3.1.2.13. Phase diagram of the pseudo-binary $BaBi_2B_4O_{10}$ – BaB_4O_7 system

The same picture is observe for $BaBi_2B_4O_{10}$ – BaB_4O_7 system: simple eutectic E_{16} is formed between two congruent melted compounds. Pseudo-binary eutectic E_{16} content 24 mol% of BaB_4O_7 and has melting point 715°C (Fig. 16).

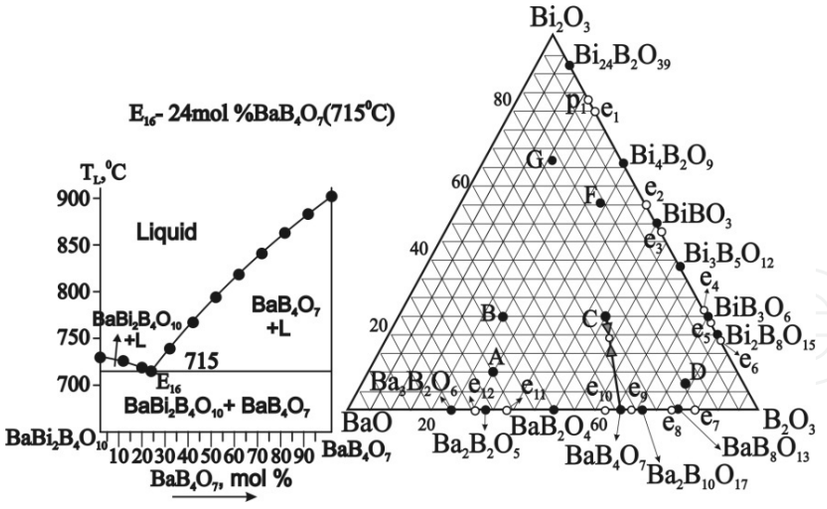

Figure 16. Phase diagram of the pseudo-binary system $BaBi_2B_4O_{10} – BaB_4O_7$.

3.1.2.14. Phase diagram of the pseudo-binary $BaBiB_{11}O_{19} – BaB_8O_{13}$ system

It is simple system with pseudo-binary eutectic E_{17} between two congruent melted $BaBiB_{11}O_{19}$ and BaB_8O_{13} compounds. Eutectic E_{17} content 38 mol% of BaB_8O_{13} and has melting point 770°C (Fig. 17).

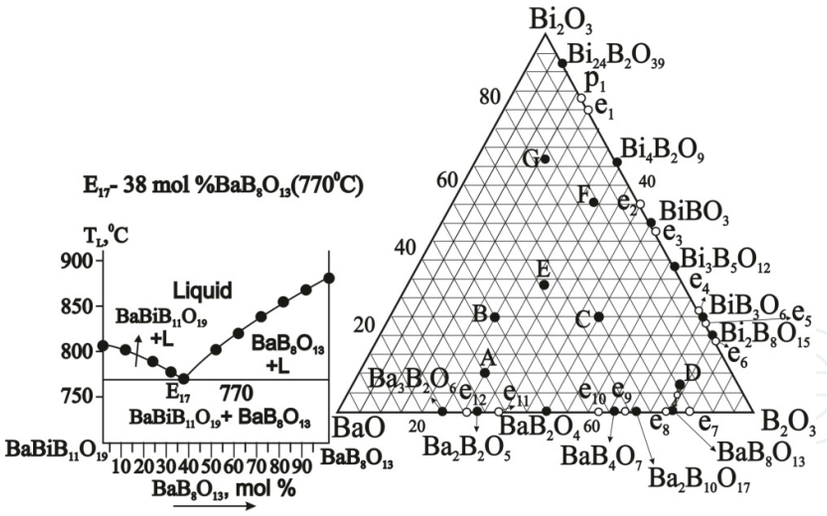

Figure 17. Phase diagram of the pseudo-binary system $BaBiB_{11}O_{19} – BaB_8O_{13}$.

3.1.2.15. Phase diagram of the $BaO-Bi_2O_3-B_2O_3$ ternary system

As result of huge work under project the phase diagram in the ternary $BaO-B_2O_3-Bi_2O_3$ system has been constructed for the first time and presented on Fig.18. Three new compounds $BaBi_2B_2O_7$, $BaBi_{10}B_6O_{25}$ and $BaBi_8B_2O_{16}$ have been revealed and characterized.

http://dx.doi.org/10.5772/52405

Fields of binary bismuth and barium borates as well as all ternary barium bismuth borates compounds crystallizations have been determined and outlined and sixteen ternary eutectic points E_1-E_{16} have been revealed as result of phase diagram construction (Fig. 18, table 3). The phase diagram evidently represents interaction of binary and ternary compounds taking place in the pseudo-ternary systems. The ternary eutectic E_1 with m.p 590°C has been determined among $BiBO_3$, F and $Bi_4B_2O_9$ compounds; ternary eutectic E_2 with m.p. 585°C has been formed among $BiBO_3$, F and C compounds; ternary eutectic E_3 with m.p. 640°C has been formed among F, E and C compounds; ternary eutectic E_4 with m.p. 622°C has been formed among C, BaB_2O_4 and E compounds; ternary eutectic E_5 with m.p. 610°C has been formed among $BiBO_3$, C and $Bi_3B_5O_{12}$ compounds; ternary eutectic E_6 with m.p. 675°C has been formed among C, $Bi_3B_5O_{12}$ and D compounds; ternary eutectic E_7 with m.p. 680°C has been formed among $Bi_3B_5O_{12}$, D and BiB_3O_6 compounds; ternary eutectic E_8 with m.p. 675°C has been formed among BiB_3O_6, D and $Bi_2B_8O_{15}$ compounds; ternary eutectic E_9 with m.p. 680°C has been formed among $Bi_2B_8O_{15}$, D and B_2O_3 compounds; ternary eutectic E_{10} with m.p. 730°C has been formed among BaB_8O_{13}, D and B_2O_3 compounds; ternary eutectic E_{11} with m.p. 750 °C has been formed among $Ba_2B_{10}O_{17}$-D- BaB_8O_{13} compounds; ternary eutectic E_{12} with m.p. 680°C has been formed among C, $Ba_2B_{10}O_{17}$ and D compounds; ternary eutectic E_{13} with m.p. 690°C has been formed among $Ba_2B_{10}O_{17}$, C and BaB_4O_7 compounds; ternary eutectic E_{14} with m.p. 700°C has been formed among BaB_4O_7, C and BaB_2O_4 compounds; ternary eutectic E_{15} with m.p. 645 °C has been formed among G, F and C compounds; ternary eutectic E_{16} with m.p. 615°C has been formed among $Bi_{24}B_2O_{39}$, F and $Bi_4B_2O_9$ compounds (Fig18, Table 3).

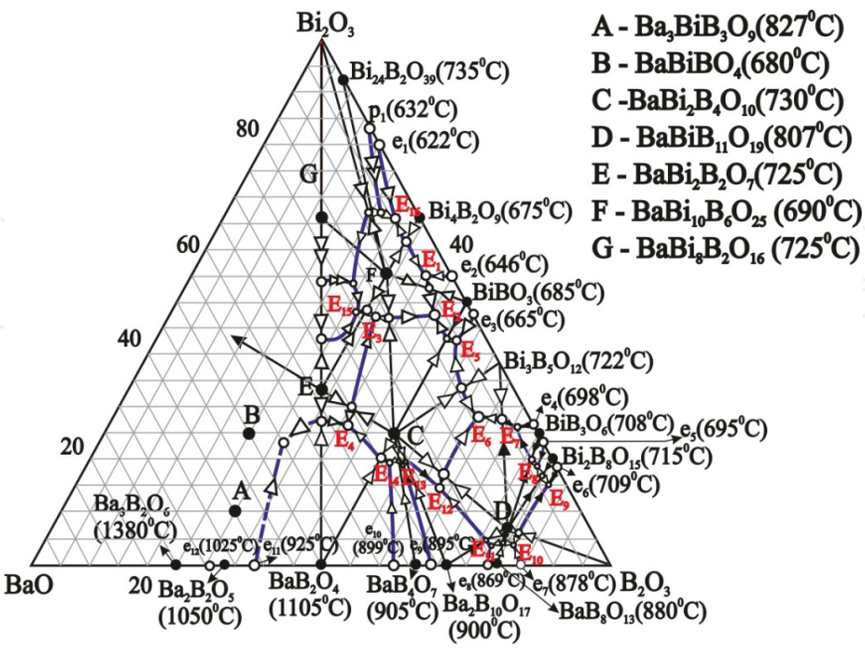

Figure 18. Phase diagram of the BaO-Bi_2O_3-B_2O_3 system

Point	Composition, mol%			T_m, °C
	BaO	B_2O_3	Bi_2O_3	
E_1	4.5	40.5	55	590
E_2	7.3	45.1	47.6	585
E_3	15	38	47	640
E_4	32.4	41.3	26.3	622
E_5	5.4	52	42.6	610
E_6	9	63	28	675
E_7	3	71	26	680
E_8	3.5	78	18.5	675
E_9	3.2	81.8	15	680
E_{10}	15	81.2	3.8	730
E_{11}	18.9	77.5	3.6	750
E_{12}	22.4	63.2	14.4	680
E_{13}	26.6	54.7	18.7	690
E_{14}	28.8	52	19.2	700
E_{15}	20	32	48	645
E_{16}	4.5	30	65.5	615

Table 3. The temperature and compositions for ternary eutectic points in the BaO-Bi_2O_3-B_2O_3 system

3.2. DTA and X-ray characterisation of ternary stoichiometric glasses and glass ceramics from the BaO-Bi_2O_3-B_2O_3 system

The glasses corresponding to known sixth stoichiometric compounds in the BaO-Bi_2O_3-B_2O_3 system examined in the present study and following glass compositions (mol%) have been melted: $14.28BaO•7.14Bi_2O_3•78.57B_2O_3$ ($BaBiB_{11}O_{19}$), $25BaO•25Bi_2O_3•50B_2O_3$($BaBi_2B_4O_{10}$), $33.33BaO•33.33Bi_2O_3•33.33B_2O_3$($BaBi_2B_2O_7$), $11.11BaO•55.55Bi_2O_3•33.33B_2O_3$ ($Bi_{10}B_6O_{25}$), $50BaO•25Bi_2O_3•25B_2O_3$ ($BaBiBO_4$) and $60BaO•10Bi_2O_3•30B_2O_3$ ($Ba_3BiB_3O_9$). These glasses DTA curves are shown in Fig. 19, giving the peaks due to the glass transition, crystallization, melting, and liquidus temperatures. The glass characteristics points T_g (glass transition), T_s(glass softening), T_c (peak of exothermal effects connected with crystalline phases crystallizations) and T_m (minimum of endothermic effects associated with these phases melting) observed on DTA curves (Fig. 19, curves 1-6) of all tested powder samples summarized on table 4.

http://dx.doi.org/10.5772/52405

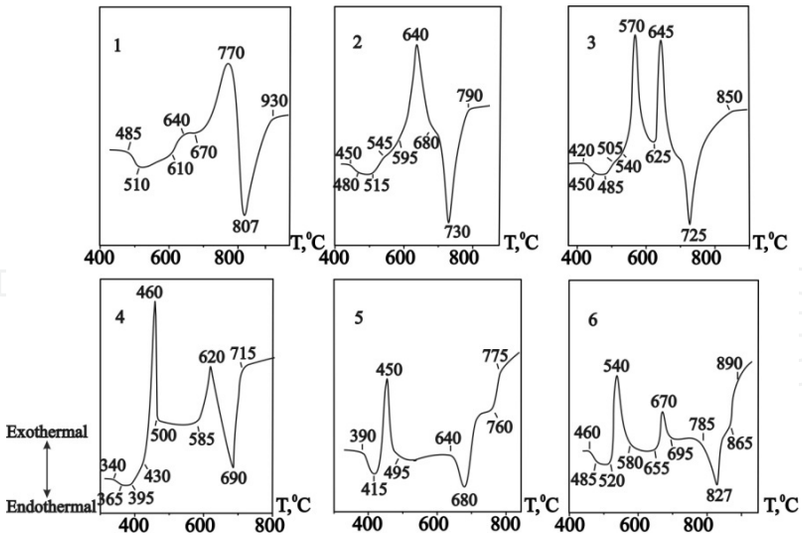

Figure 19. DTA curves (heating rate 10K/min) of glasses corresponding to ternary compounds in the BaO-Bi_2O_3-B_2O_3 system: 1-$BaBiB_{11}O_{19}$, 2-$BaBi_2B_4O_{10}$, 3-$BaBi_2B_2O_7$, 4-$BaBi_{10}B_6O_{25}$,5-$BaBiBO_4$, 6-$Ba_3BiB_3O_9$.

##	Glass compositions, correspoding to stoichometric compounds	Dilatometric characteristics			DTA characteristics			
		TEC(α_{20-300})•10^7K^{-1}	T_g,°C	T_s ,°C	T_g, °C	T_{cr}, °C	T_m, °C	T_L, °C
1	$BaBiB_{11}O_{19}$ (glass)	72	498	535	485	640; 770	807	807
	$BaBiB_{11}O_{19}$ (615°C 24h)	49.8						
2	$BaBi_2B_4O_{10}$ (glass)	96	445	475	450	545; 640	730	730
	$BaBi_2B_4O_{10}$ (640°C 24h)	77.9						
3	$BaBi_2B_2O_7$ (glass)	108	415	455	420	570; 645	725	725
	$BaBi_2B_2O_7$ (640°C 24h)	96						
4	$BaBi_{10}B_6O_{25}$ (glass)	99	350	380	340	460; 620	690	690
	$BaBi_{10}B_6O_{25}$(590°C 24h)	97						
5	$BaBiBO_4$ (glass)	120	400	450	390	450	680	760
	$BaBiBO_4$ (570°C 24h)	110.8						
6	$Ba_3BiB_3O_9$ (glass)	127	460	490	460	540; 670	827	865
	$Ba_3BiB_3O_9$ (690°C 24h)	109.8						

Table 4. Chemical compositions, DTA (glass transition -T_g, crystallization peak -T_{cr}, melting -T_m, liquidus- T_L) and dilatometric characteristics (glass transition temperature -T_g, softening point - T_S, thermal expansion coefficient -TEC) of BaO-Bi_2O_3-B_2O_3system glasses and crystallaised glasses.

Two exothermic effects were observed on DTA curve of 14.28BaO•7.14Bi_2O_3•78.57B_2O_3 (mol %) glass composition: first weak effect at 640°C and second strong effect at 770°C(Fig.19,

curve1). The melting temperature (T_m) is equal to 807°C and corresponding to Egorisheva and Kargin's data [30]. X-ray patterns of this glass crystallization products show one $BaBiB_{11}O_{19}$ crystalline phase presence [30], which formed at powder samples crystallization in an temperature interval 640-770°C (Fig.20, curve1). It is possible to assume, that weak exothermic effect at 640°C apparently is connected with pre-crystallisation fluctuations taking place in glass matrix [50]. Diffuse character of second exothermic effect at 770°C testifies about dominating surface crystallisation of the given glass particles.

One sharp exothermic effect at 640°C and sharp endothermic effect at 730°C were observed on DTA curve of $BaBi_2B_4O_{10}$ glass composition (Fig. 19, curve2). The melting temperature (T_m) is equal to 730°C and corresponding to Egorisheva's data [30]. X-ray diffraction patterns of this glass crystallization products show one $BaBi_2B_4O_{10}$ crystalline phase crystallization[30], which formed at glass powder samples crystallization at temperature 640°C (Fig. 20, curve2) and its melting. T_m is equal to 730°C and corresponding to Egorisheva's data [30]. Hardly visible pre-crystallisation fluctuation exothermal effect is observed also at 545°C (Fig. 19, curve2).

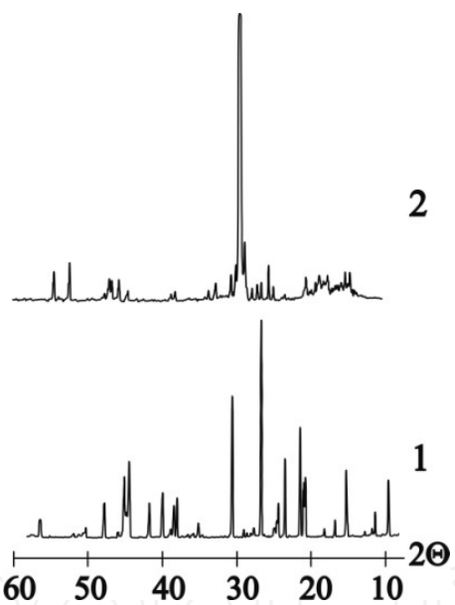

Figure 20. XRD-patterns of the crystallized glasses corresponding to ternary $BaBiB_{11}O_{19}$ (1- 760 °C 24h,cooling in the muffle) and $BaBi_2B_4O_{10}$ (2- 640°C 24h,cooling in the muffle) compounds

On the DTA curves of stoichiometric $BaBi_2B_2O_7$ and $BaBi_{10}B_6O_{25}$ glass compositions observed two exothermal effects at 570 and 645°C for $BaBi_2B_2O_7$ and at 460 and 620°C for $BaBi_{10}B_6O_{25}$ (Fig. 19, curves 3,4). But both compositions have one endothermic effect of melting at 725 and 690°C respectively for $BaBi_2B_2O_7$ and $BaBi_{10}B_6O_{25}$ testifying to one formed crystalline phase melting (Fig. 19, curves 3,4). X-ray data of these samples confirmed monophase crystallizations in each samples (Fig. 21, curves 1,2; Fig.22, curves 1,2).

According to [34] the X-ray powder diffraction patterns of formed $BaBi_2B_2O_7$ crystalline phase at stoichiometric glass composition ($33.33BaO \bullet 33.33Bi_2O_3 \bullet 33.33B_2O_3$ mol%) at second

http://dx.doi.org/10.5772/52405

exothermic peaks temperature (640°C 24h) was indexed on an orthorhombic cell with following lattice parameters: a=11.818Å, b=8.753 Å, c=7.146Å, cell volume V=739.203 Å, Z=4 (Fig. 21, curve2). XRD-patterns of products of same glass crystallization at 570°C 24h keeps all diffraction lines of its analogue obtained at 640°C 24h (Fig. 21, curve1). Difference is observed only in sharp increasing of intensity (I/I_o) of [030] diffraction line from 4 to 43 at high temperature crystallization. That leads to reorientation of crystal structure, decreasing [030] diffraction line and accompanied with occurrence of the second exothermal effect on DTA curve (Fig. 19, curve 3).

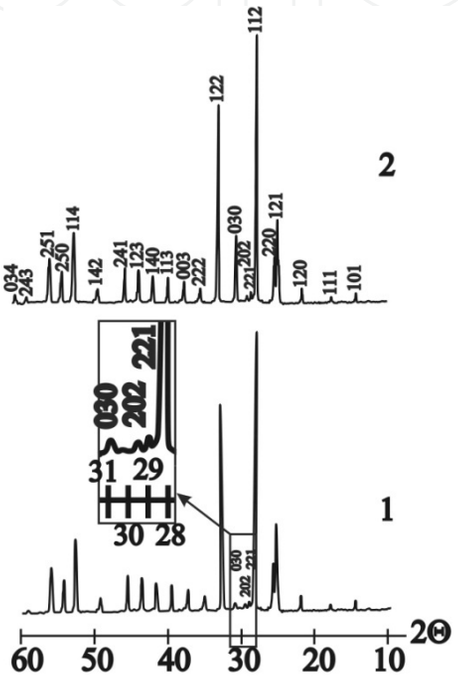

Figure 21. XRD-patterns of the crystallized glasses corresponding to ternary $BaBi_2B_2O_7$ composition:

1-570°C 24h, cooling in the muffle; 2-640°C 24h, casting in the cold water

X-ray powder diffraction patterns of $BaBi_{10}B_6O_{25}$ single crystals was indexed on an orthorhombic cell with following lattice parameters: a=6.434Å, b=11.763 Å, c=29.998Å, cell volume V=2270.34 Å, Z=8 [34]. XRD-patterns of products of same compositions (11.11BaO• 55.55Bi_2O_3• 33.33B_2O_3 mol%) glass crystallization at both exothermal effects (420°C 24h and 620°C 24h) have all diffraction lines of the $BaBi_{10}B_6O_{25}$ single crystals (Fig. 22, curves1-3). Naturally, $BaBi_{10}B_6O_{25}$ single crystal has well generated planes and clear observed diffraction lines on XRD-patterns in contrast to crystalline phases formed at same composition glasses crystallization. However, the most intensive diffraction line (I/I_o=100) of single crystals is [133], whereas products of glass crystallizations have [203] strongest diffraction line and [133] diffraction line became 5-10 times less (Fig. 22, curves1-3). Now it is difficult to us only on the basis of XRD-patterns analysis of glass crystallizations products to assume the nature of the second exothermal effect at 620°C on DTA curve of $BaBi_{10}B_6O_{25}$ of glass composition (Fig.19, curve 4). Their XRD-patterns are identical each other and to single crystals,

but contain slightly quantity of not indexed reflexes, which are absent in X-ray powder diffraction patterns of $BaBi_{10}B_6O_{25}$ single crystals (Fig. 22, curves1-3).

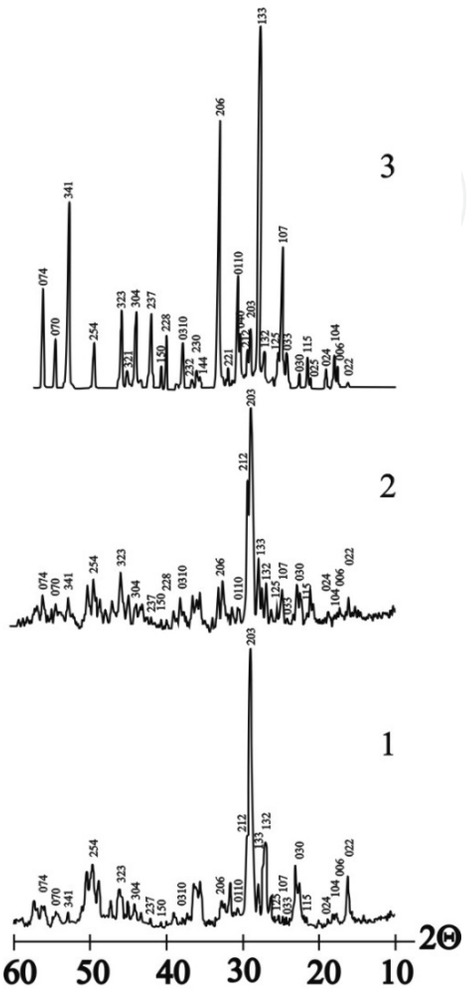

Figure 22. XRD-patterns of the crystallized glasses corresponding to ternary $BaBi_{10}B_6O_{25}$ composition:(1-460°C 24h,cooling in the muffle; 2-620°C 24h, casting in the cold water) and $BaBi_{10}B_6O_{25}$ single crystals (3).

The DTA curve of 50BaO• $25Bi_2O_3$• $25B_2O_3$ mol% ($BaBiBO_4$) glass composition contain exothermal effect of glass crystallization at 450°C and endothermic effect of this crystalline phase melting at 680°C (Fig. 19, curv.5). X-ray diffraction patterns of this glass crystallization products show one $BaBiBO_4$ crystalline phase formation at glass powder samples crystallization at temperature interval 450-640°C(Fig. 23, curve 1), which completely correspond to Barbier with co-authors data [29]. A second endothermic effect within the interval of 745-775°C with minimum at 760°C is associated with $BaBiBO_4$ incongruent melting (Fig. 19, curve 5).

We have revealed also, that the crystalline $BaBiBO_4$ compound is melted incongruently at 680°C with the melt and crystalline $BaBiO_3$ formation (Fig. 23, curve 2). The $BaBiO_3$ crystalline phase was observed on XRD-patterns of thermal treated at 720 °C and fast freeze in cold

http://dx.doi.org/10.5772/52405

water products and identified according to X-ray database [43, fail # 01-074-7523]. The dissolution of this $BaBiO_3$ phase in a melt leads to the appearance on a DTA curve the second endothermic effect in an interval 745-775°C (Fig. 19, curve 5). Above 775°C we have glass-forming $BaBiBO_4$ composition melt without presence of any crystalline phase.

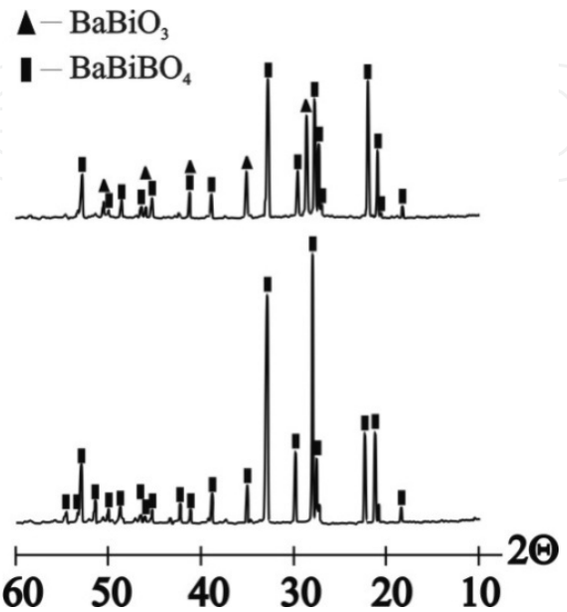

Figure 23. XRD-patterns of the crystallized glasses corresponding to ternary $BaBiBO_4$ composition:

1-450°C 24h, cooling in the muffle; 2-720°C 3h, casting in the cold water

Two exothermal effects of glass crystallization at 540 and 670°C and one endothermic effect of crystalline phase melting at 827°C are seen on the DTA curve of the $60BaO•10Bi_2O_3•30B_2O_3$ mol% ($Ba_3BiB_3O_9$) glass composition (Fig. 19, curve 6). X-ray diffraction patterns of this glass crystallization products at 540 and 670°C show one $Ba_3BiB_3O_9$ crystalline phase formation (Fig. 24, curves 1,2) at glass powder samples crystallization at 540 and 670°C and fully correspond to Egorisheva with co-authors data, which synthesized for the first time and have describe $Ba_3BiB_3O_9$ compound [31]. However, we didn't indicate polymorphic transition of $Ba_3BiB_3O_9$ at 850°C as reported in [31]. Presence of second endothermic effect within the interval of 840-890°C with minimum at 865°C is associated with $Ba_3BiB_3O_9$ incongruent melting (Fig. 19, curve 6). We have revealed that the crystalline $Ba_3BiB_3O_9$ compound is melted incongruently at 827°C with the glass forming melt and crystalline phase formation (Fig. 24, curve 3). The $Ba_2B_2O_5$ crystalline phase was observed in amorphous matrix on XRD-patterns of thermal treated at 830 °C and fast freeze in cold water products and identified according to X-ray database [43, fail # 024-0087]. For clear $Ba_2B_2O_5$ observation on XRD-patterns the preliminary crystallized at 670°C 24h sample have been exposed at 830°C 3 h (Fig. 23, curve3). Dissolution of this $Ba_2B_2O_5$ phase in a melt leads to the appearance on a DTA curve the second endothermic effect in an interval 840-890°C (Fig. 19, curve 6). Above 890°C we have glass-forming $Ba_3BiB_3O_9$ composition melt without presence of any crystalline phase at cooling rate 10^2 K/s.

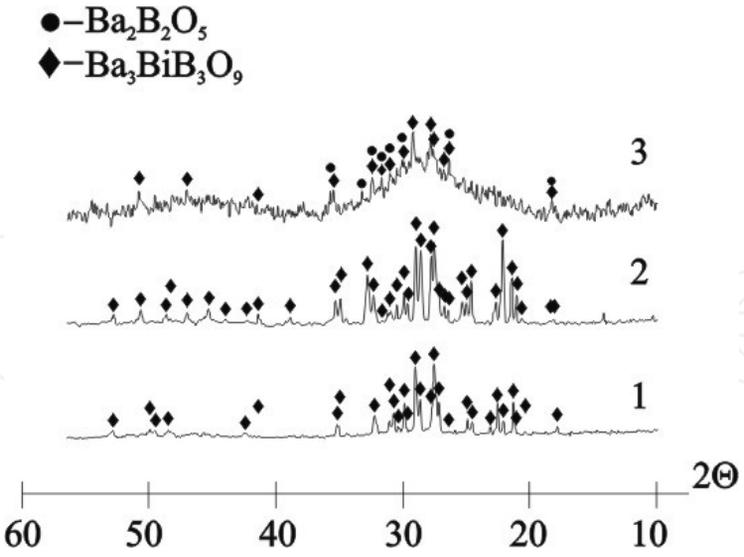

Figure 24. XRD-patterns of the crystallized glasses corresponding to ternary $6BaBi3BO_4$ composition:1.540°C 24h, cooling in the muffle; 2-670°C 24h, casting in the cold water; 3-670°C 24h+830°C 3 h, casting in the cold water

3.3. TEC study of the stoichiometric compositions glasses in the $BaO\text{-}Bi_2O_3\text{-}B_2O_3$ system

The isolines diagram of $BaO\text{-}Bi_2O_3\text{-}B_2O_3$ system glasses TEC values is given on Fig. 25. It is clear observed common regularity, that the increase of barium and bismuth oxides amounts in glasses of binary $BaO\text{-}Bi_2O_3$ and $Bi_2O_3\text{-}B_2O_3$ systems leads to increase TEC of glasses. The same tendency is observed for glasses of ternary system: joint presence of BaO and Bi_2O_3 and increase their amounts leads to increase glasses TEC values from 70 to $127 \bullet 10^{-7}K^{-1}$ (Fig. 25).

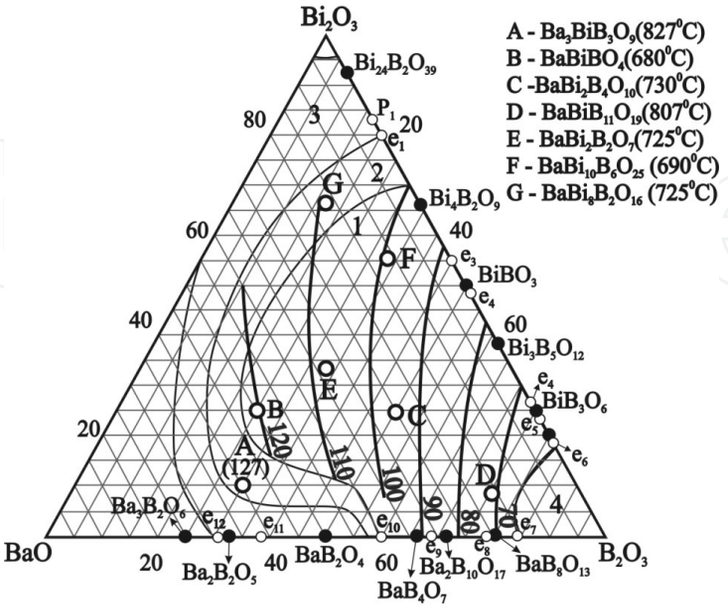

Figure 25. $BaO\text{-}Bi_2O_3\text{-}B_2O_3$ system's glasses TEC ($\alpha_{20\text{-}300} \bullet 10^{-7}K^{-1}$) values isolines

http://dx.doi.org/10.5772/52405

The high boron content glass composition corresponds to $BaBiB_{11}O_{19}$ (14.28BaO•7.14Bi_2O_3•78.57B_2O_3 mol %) have TEC=72•$10^{-7}K^{-1}$ and T_g=498°C calculated from dilatometric curve (Table 4). Reduction the B_2O_3 amount together with increasing of BaO and Bi_2O_3 amounts in glass compositions leads to increase TEC and reduction Tg values: for glass composition 25BaO•25Bi_2O_3•50B_2O_3 mol % ($BaBi_2B_4O_{10}$) TEC=96•$10^{-7}K^{-1}$ and T_g= 445°C; 33.3BaO•33.3 Bi_2O_3•33.3B_2O_3 mol %($BaBi_2B_2O_7$) TEC=108•$10^{-7}K^{-1}$ and T_g=415°C; 11.1BaO• 55.5Bi_2O_3•33.3B_2O_3 mol %($BaBi_{10}B_6O_{25}$) TEC=97•$10^{-7}K^{-1}$ and T_g=350°C; 16.67BaO•66.67Bi_2O_3•16.67B_2O_3 mol%($BaBi_8B_2O_{16}$) TEC=110•$10^{-7}K^{-1}$ and T_g=415°C. However, for 50BaO•25 Bi_2O_3•25B_2O_3 mol % ($BaBiBO_4$) and 60BaO•10Bi_2O_3•30B_2O_3 mol % ($Ba_3BiB_3O_9$) glass compositions simultaneous increase both TEC and T_g values were observed: TEC=120•$10^{-7}K^{-1}$ and T_g=400°C; TEC=127•10^{-7} K^{-1} and T_g=460°C respectively for $BaBiBO_4$ and $Ba_3BiB_3O_9$ (Fig. 25, table4).

TEC values of crystallized glasses corresponding to the ternary barium bismuth borates given in Table 4. Crystallized barium bismuth borate glass samples have TEC values lower, than initial glasses and equals to: 49•$10^{-7}K^{-1}$ for $BaBiB_{11}O_{19}$ sample (750°C 24h), 78•$10^{-7}K^{-1}$ for $BaBi_2B_4O_{10}$ sample (630°C 24 h), 96•10^{-7} K^{-1} for $BaBi_2B_2O_7$ sample (640°C 24h), 97•$10^{-7}K^{-1}$ for $BaBi_{10}B_6O_{25}$ sample (610°C 24h), 110•10^{-7} K^{-1} for $BaBiBO_4$ sample (450°C24h) and 109•10^{-7} K^{-1} for $Ba_3BiB_3O_9$ sample (690°C 24h). The same tendency, as well as for their glassy analogues, is observed for crystallized glass samples: increase of barium and bismuth oxides amounts in ternary compounds leads to their TEC values increase.

4. Ferroelectric properties of new ternary $BaBi_2B_2O_7$ and $BaBi_{10}B_6O_{25}$ stoichometric compositions glass ceramics.

The ferroelectric (polarization - electric field) hysteresis, is a defining property of ferroelectric materials. Thus, the most widely studied characteristics of ferroelectric hysteresis were those of interest for this particular application: the value of the switchable polarization (the difference between the positive and negative remanent polarization, $P_R - (-P_R)$, dependence of the coercive field *Ec* on sample thickness, decrease of remanent or switchable polarization with number of switching cycles, polarization imprint, endurance, retention [51].

Electric field induced polarization (P) and remanent polarization(P_r) were measured at room temperature for $BaBi_2B_2O_7$ and $BaBi_{10}B_6O_{25}$ glass tape samples crystallized using various regimes (Fig. 26).

a. $BaBi_2B_2O_7$ glass tape sample of 0.07 mm in thickness crystallized at 450°C 24h, $2P_r$ = 0.15 μC/cm^2;

b. $BaBi_{10}B_6O_{25}$ glass tape sample of 0.06 mm in thickness crystallized at 380 °C 12h, $2P_r$ = 0.32 μC/cm^2;

c. $BaBi_{10}B_6O_{25}$ glass tape sample of 0.06 mm in thickness crystallized at 410°C 12h, $2P_r$ = 0.62 μC/cm^2;

d. $BaBi_{10}B_6O_{25}$ glass tape sample of 0.05 mm in thickness crystallized at 410°C 24h, $2P_r$ = 0.9 μC/cm^2

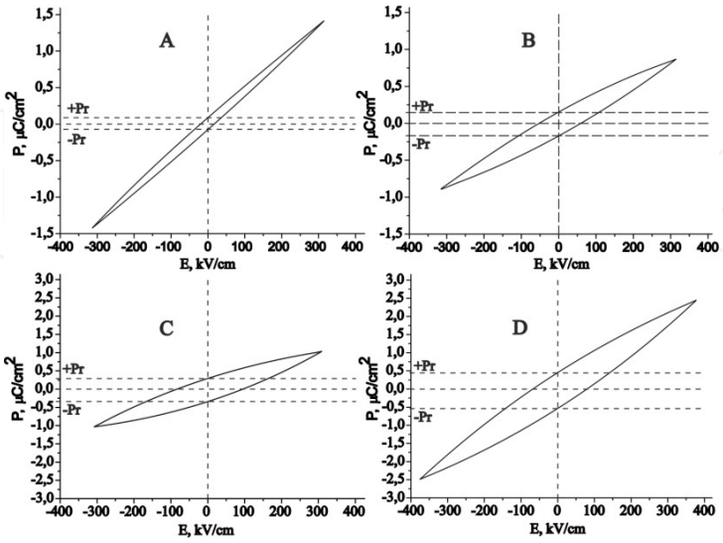

Figure 26. Dependence of polarization (P) on electric field (E) for crystallized stoichiometric glass compositions:

Linear *P–E* curves are observed up to fields of 40-120 kV/cm for all measured samples with thickness 0.05-0.07mm. The polarization becomes nonlinear with increasing of applied electric field, and at 140-380 kV/cm the remanent polarization $2P_r$ values were found 0.15 μC/cm^2 for the $BaBi_2B_2O_7$ (Fig. 26, A). The remanent polarization $2P_r$ value for $BaBi_{10}B_6O_{25}$ crestallized glass tape samples encreasing with termal treatment temperature from 0,32 to 0, 64 μC/cm^2 (Fig. 26, B & C) and time (Fig. 26, D). The highest remanent polarization value ($2P_r$=0.9 μC/cm^2) has $BaBi_{10}B_6O_{25}$ glass tape sample crystallized at 410°C 24h (Fig.26, D). According to obtained results it is possible to conclude that samples are ferroelectrics.

5. Discussion

The pricipial diference of our methodology from traditional is a glass samples using as initial testing substance for phase diagram of very complex ternary $BaO\text{-}Bi_2O_3\text{-}B_2O_3$ system construction. It is a very effective method, due possibility to indicate temperature intervals of all processes taking place in glass samples: glass transition, crystallization, quantity of formed crystalline phases and their melting. Whereas, samples prepared by traditional solid phase synthesis are less informative and often lose a lot of information. Super cooling technique created by our group allowed us both to expand borders of glass formation and to have enough quantity samples for DTA and X-ray investigations and $BaO\text{-}Bi_2O_3\text{-}B_2O_3$ system phase diagram construction (Fig.2).

The region of stable glasses includes the binary compounds BaB_4O_7, $Ba_2B_{10}O_{17}$, BaB_8O_{13}, $Bi_4B_2O_9$, $BiBO_3$, $Bi_3B_5O_{12}$, BiB_3O_6, and $Bi_2B_8O_{15}$ in the $BaO–B_2O_3$ and $Bi_2O_3–B_2O_3$ systems (Fig.

http://dx.doi.org/10.5772/52405

2). Binary BaB_4O_7, $Ba_2B_{10}O_{17}$, and BaB_8O_{13} barium borates have melting temperatures (Tm) of 910, 905, and 890°C and can be found between the eutectics e_7, e_8, e_9, and e_{10} with Tm = 878, 869, 895, and 899°C, respectively. The transition to a crystallization field of barium metaborate is accompanied by a sharp increase of liquidus temperature (T_L) and a decrease of the glass forming ability of the melts. The final compound, forming a stable glass, contains ~43 mol %BaO and has T_L = 950°C. Compounds BaB_2O_4 and $Ba_2B_2O_5$, having higher Tm, which are 1095 and 1050°C, respectively [18, 21, 22], are found in the region of the compounds obtained in the form of glasses with a cooling rate of (10^3–10^4) K/s. Glass formation in the BaO–B_2O_3 binary system is limited by the eutectic e_{12} with Tm = 1025°C (Fig. 2) because of the sharp increase of the liquidus temperature during the transition to a field of crystallization of the $Ba_3B_2O_6$ compound (Tm = 1383°C). BaB_2O_4 (Tm = 1095°C) is the dominating compound in the system and does not form stable glasses. Its considerable crystallization field narrows the region of stable glasses in the ternary system, which is only restricted by compounds with T_L ~ 950°C (Fig. 2).

Binary bismuth borates $Bi_4B_2O_9$, $BiBO_3$, $Bi_3B_5O_{12}$, BiB_3O_6, and $Bi_2B_8O_{15}$ have Tm 675, 685, 722, 708, and 715°C can be found between the eutectics e_1, e_2, e_3, e_4, e_5, e_6 with a Tm of 622, 646, 665, 698, 695, and 709°C, respectively [2, 34]. The region of stable glasses in the Bi_2O_3–B_2O_3 system is limited by a compound containing ~70%mol Bi_2O_3 and having T_L = 670°C. Compounds that are found in the range of 70–80mol% Bi_2O_3 (before the e_1 point) are obtained in the form of glasses during cooling at a rate of ~10^2 K/s. During the transition to the crystallization field of $Bi_{24}B_2O_3$ and Bi_2O_3, T_L increases to 825°C (Tm of Bi_2O_3). Glasses in this part of the system are obtained during melt cooling at a rate of (10^3–10^4) K/s. These compounds have a low liquidus temperature; however, the structure factor essentially influences their glass forming ability, not allowing glass formation at low melt cooling rates.

Six ternary compounds are known in the BaO–Bi_2O_3–B_2O_3 system: $Ba_3BiB_3O_9$, $BaBiBO_4$, $BaBi_2B_4O_{10}$, and $BaBiB_{11}O_{19}$ synthesized by Barbie and Egorysheva in 2005–2006, and $BaBi_2B_2O_7$ and $BaBi_{10}B_6O_{25}$ revealed by our research group in 2008–2009. $BaBi_2B_4O_{10}$, $BaBiB_{11}O_{19}$, $BaBi_2B_2O_7$, and $BaBi_{10}B_6O_{25}$ melt congruently at 730, 807, 725, and 695°C respectively, and $BaBiBO_4$ melts incongruently at 680°C and has T_L = 760 °C. All these five ternary compounds along with the eutectics formed between each other and with binary barium and bismuth borates form a "plateau" with low T_L, which is responsible for the formation of the region of stable glasses in the ternary system BaO–Bi_2O_3–B_2O_3.

Compounds joining low temperature eutectic e_1 (622°C) [2] in the Bi_2O_3–B_2O_3 binary system and the eutectics e_{13} (~790°C) and e_{14} (~750°C) in the BaO–Bi_2O_3 binary system 26 - 28] form glasses only at higher cooling rates of their melts (10^3–10^4) K/s. Glass formation in the BaO–Bi_2O_3 binary system stops at 45 mol% BaO content (T_L ~930°C) [26 - 28]. Along with the factor of the liquidus temperature [52], a considerable contribution to the glass formation of the pointed compositions is made by the structural factor of the melt. The combination of the structural factors of the melt and the liquidus temperature is also considerable during the transition to the vitreous state of the compositions, which are found in the crystallization fields of BaB_2O_4 and $Ba_2B_2O_5$, where they show the tendency towards glass formation only at high rates of melt cooling.

There are very stable congruent melted binary BaB_2O_4 and ternary $BaBi_2B_4O_{10}$, $BaBiB_{11}O_{19}$, and $BaBi_{10}B_6O_{25}$ compounds in the studied ternary $BaO\text{-}Bi_2O_3\text{-}B_2O_3$ system. They have dominating positions in ternary diagram and occupied the biggest part of it (Fig.18). Mutual influence of these compounds and other binary and ternary compounds (BaB_4O_7, $Ba_2B_{10}O_{17}$, BaB_8O_{13}, $Bi_4B_2O_9$, $BiBO_3$, $Bi_3B_5O_{12}$, BiB_3O_6, $Bi_2B_8O_{15}$, $BaBi_2B_2O_7$, and $BaBi_8B_2O_{16}$) lead to formation of sixteen revealed at present time ternary eutectics (Fig.18& Table 3), which have essential influence on liquidus temperature decrease and to assist in glass formation. Ternary $BaBi_2B_4O_{10}$ compound forms eight eutectics with binary and ternary compounds, its neighbors: E_4(622°C), E_3(640°C), E_2(585°C), E_5(610°C), E_6(675°C), E_{12}(680°C), E_{13} (690°C), and E_{14} (700°C) (Fig.18& Table 3). $BaBiB_{11}O_{19}$ compound forms seven eutectics with its neighbors: E_6 (675°C), E_7 (680°C), E_8 (675°C), E_9 (680°C), E_{10} (730°C), E_{11} (750°C),and E_{12} (680°C) (Fig.18& Table 3). $BaBi_{10}B_6O_{25}$ compound forms five eutectics with its neighbors: E_1 (590°C), E_2 (585°C), E_3 (640°C), E_{15} (645°C), and E_{16} (615°C) (Fig.18& Table 3). Determined ternary eutectics together with binary eutectics e_1, e_2, e_3, e_4, e_5, and e_6 of $Bi_2O_3\text{-}B_2O_3$ system have allowed to outline the fields of binary $Bi_4B_2O_9$, $BiBO_3$, $Bi_3B_5O_{12}$, BiB_3O_6, and $Bi_2B_8O_{15}$ bismuth borates crystallisation, as well as together with binary eutectics e_7, e_8, e_9, and e_{10} of $BaO\text{-}B_2O_3$ system have allowed to outline the fields of binary BaB_4O_7, $Ba_2B_{10}O_{17}$, BaB_8O_{13} barium borates and partly BaB_2O_4 crystallization on the $BaO\text{-}Bi_2O_3\text{-}B_2O_3$ system phase diagram (Fig.18).

The clear correlation between glass forming and phase diagrams has been observed in studied system. The glass melting temperature and level of glass formation depending on the cooling rate of the studied melts are in good conformity with boundary curves and eutectic points (Fig.2& 18).

The phase diagram of the well known binary Bi_2O_3–B_2O_3 system has been corrected in the interval between the $Bi_4B_2O_9$ and $Bi_3B_5O_{12}$ compounds. The eutectic composition, $48.5Bi_2O_3 \bullet 51.5B_2O_3$ (mol%), between $BiBO_3$ and $Bi_3B_5O_{12}$, with m.p. 665±5°C, has been determined. It is shown that the compound $BiBO_3$ is congruently melting with a m.p. of 685±5°C.

The next unexpected results were obtained at phase diagram construction: two new ternary $BaBi_2B_2O_7$ and $BaBi_{10}B_6O_{25}$ compounds have been revealed at the same glass compositions crystallisation. X-ray characteristics of the new ternary compound $BaBi_2B_2O_7$, synthesized at the $33.33BaO \bullet 33.33Bi_2O_3 \bullet 33.33B_2O_3$ (mol%) glass composition crystallization at 640°C, 20 h. The x-ray powder diffraction patterns of $BaBi_2B_2O_7$ could be indexed on an orthorhombic cell with lattice parameters as follows: $BaBi_2B_2O_7$ a=11.818 Å, b=8.753 Å, c=7.146 Å, cell volume V=739.203 Å^3, Z=4.

Single crystals of $BaBi_{10}B_6O_{25}$ were obtained by cooling of a melt with the stoichiometric composition. Glass powder of composition $11.11BaO \bullet 55.55Bi_2O_3 \bullet 33.33B_2O_3$ (mol%) was heated in a quartz glass ampoule up to 750°C at a rate 10 K/min. After 2 h at high temperature, the melt was cooled at a rate 0.5 K/h. Single crystals with sizes up to 1.66×0.38×0.19 mm^3 were grown. The x-ray powder diffraction patterns of $BaBi_{10}B_6O_{25}$ could be indexed on an orthorhombic cell with lattice parameters as follows: a=6.434 Å, b=11.763 Å, c=29.998 Å, cell volume V=2270.34 Å^3, Z=8.

http://dx.doi.org/10.5772/52405

Common regularities of bulk glass samples TEC changes in studied $BaO-Bi_2O_3-B_2O_3$ system have been determined: the increase of barium and bismuth oxides amounts in glasses of binary $BaO-Bi_2O_3$ and $Bi_2O_3-B_2O_3$ systems leads to increase TEC of glasses. The same tendency is observed for glasses of ternary $BaO-Bi_2O_3-B_2O_3$system: joint presence of BaO and Bi_2O_3 and increase their amounts leads to increase glasses TEC values from 70 to $127•10^{-7}K^{-1}$ (Fig. 25).

Crystallized barium bismuth borate glass samples have TEC values lower, than initial glasses and equals to: $49•10^{-7}K^{-1}$ for $BaBiB_{11}O_{19}$ sample (750°C 24h), $78•10^{-7}K^{-1}$ for $BaBi_2B_4O_{10}$ sample (630°C 24 h), $96•10^{-7}$ K^{-1} for $BaBi_2B_2O_7$ sample (640°C 24h), $97•10^{-7}K^{-1}$ for $BaBi_{10}B_6O_{25}$ sample (610°C 24h), $110•10^{-7}$ K^{-1} for $BaBiBO_4$ sample (450°C24h) and $109•10^{-7}$ K^{-1} for $Ba_3BiB_3O_9$ sample (690°C 24h). The same tendency, as well as for their glassy analogues, is observed for crystallized glass samples: increase of barium and bismuth oxides amounts in ternary compounds leads to their TEC values increase.

Electric field induced polarization (P) and remanent polarization (P_r) were measured at room temperature for $BaBi_2B_2O_7$ and $BaBi_{10}B_6O_{25}$ glass tape samples crystallized at various regimes. All tested samples shown loop of hysteresis.

Linear *P–E* curves are observed up to fields of 40-120 kV/cm for all measured samples with thickness 0.05-0.07mm. The polarization becomes nonlinear with an increase of applied electric field, and at 140-400 kV/cm the remanent polarization $2P_r$ values were found 0.15 $\mu C/cm^2$ for the $BaBi_2B_2O_7$ (Fig.26, A), and 0.32- 0.9 $\mu C/cm^2$ for the $BaBi_{10}B_6O_{25}$ (Fig.26, B-D), crystallized glass tape samples. According to obtained results it is possible to conclude that all tested samples are ferroelectrics.

5. Conclusion

Effective way of new system investigation and new compounds and characteristic points revealing via simultaneous glass forming and phase diagrams construction have been shown. Phase diagram of the ternary $BaO-Bi_2O_3-B_2O_3$ system have been constructed for the first time us result of fourteen pseudo-binary systems and sections phase diagrams investigations.

The phase diagram of the well known binary $Bi_2O_3–B_2O_3$ system has been corrected in the interval between the $Bi_4B_2O_9$ and $Bi_3B_5O_{12}$ compounds. The eutectic composition, $48.5Bi_2O_3•51.5B_2O_3$ (mol%), between $BiBO_3$ and $Bi_3B_5O_{12}$, with m.p. 665±5°C, has been determined. It is shown that the compound $BiBO_3$ is congruently melting with a m.p. of 685±5°C.

Two new ternary $BaBi_2B_2O_7$ and $BaBi_{10}B_6O_{25}$ compounds have been revealed at the same glass compositions crystallisation. The new ternary compound $BaBi_2B_2O_7$ synthesized at the $33.33BaO•33.33Bi_2O_3•33.33B_2O_3$ (mol%) glass composition crystallization at 640°C, 20 h. The x-ray powder diffraction patterns of $BaBi_2B_2O_7$ could be indexed on an orthorhombic cell with lattice parameters as follows: $BaBi_2B_2O_7$ a=11.818 Å, b=8.753 Å, c=7.146 Å, cell volume V=739.203 $Å^3$, Z=4.

Single crystals of $BaBi_{10}B_6O_{25}$ were obtained by cooling of a melt with the stoichiometric composition. Glass powder of composition $11.11BaO•55.55Bi_2O_3•33.33B_2O_3$ (mol%) was

heated in a quartz glass ampoule up to 750°C at a rate 10 K/min. After 2 h exposition at high temperature, the melt was cooled at a rate 0.5 K/h. Single crystals with sizes up to 1.66×0.38×0.19 mm^3 were grown. The x-ray powder diffraction patterns of $BaBi_{10}B_6O_{25}$ could be indexed on an orthorhombic cell with lattice parameters as follows: a=6.434 Å, b=11.763 Å, c=29.998 Å, cell volume V=2270.34 $Å^3$, Z=8.

Ternary $BaBi_2B_4O_{10}$, $BaBiB_{11}O_{19}$, and $BaBi_{10}B_6O_{25}$ compounds have dominating positions in ternary diagram and occupied the biggest part of it. Mutual influence of these and other binary and ternary compounds (BaB_4O_7, $Ba_2B_{10}O_{17}$, BaB_8O_{13}, $Bi_4B_2O_9$, $BiBO_3$, $Bi_3B_5O_{12}$, BiB_3O_6, $Bi_2B_8O_{15}$, $BaBi_2B_2O_7$, and $BaBi_8B_2O_{16}$) lead to formation of sixteen ternary eutectics, which have essential influence on liquidus temperature decrease and to assist in glass formation.

The clear correlation between glass forming and phase diagrams has been observed: glass melting temperature and level of glass formation depending on the cooling rate of the studied melts are in good conformity with boundary curves and eutectic points.

Common regularities of bulk glass samples TEC changes in studied $BaO\text{-}Bi_2O_3\text{-}B_2O_3$ system have been determined: the increase of barium and bismuth oxides amounts in glasses of binary $BaO\text{-}Bi_2O_3$ and $Bi_2O_3\text{-}B_2O_3$ systems and their joint amounts increasing in ternary compositions leads to increase glasses TEC values from 70 to $127 \bullet 10^{-7}K^{-1}$.

Crystallized barium bismuth borate glass samples have TEC values lower, than initial glasses. Increase of barium and bismuth oxides amounts in ternary compounds leads to their TEC values increasing from 49 to $109 \bullet 10^{-7}K^{-1}$.

Electric field induced polarization (P) and remanent polarization (P_r) were measured at room temperature for $BaBi_2B_2O_7$ and $BaBi_{10}B_6O_{25}$ glass tape samples crystallized at various regimes. The remanent polarization $2P_r$ values were found 0.15 $\mu C/cm^2$ for the $BaBi_2B_2O_7$, and 0.32- 0.9 $\mu C/cm^2$ for the $BaBi_{10}B_6O_{25}$ crystallized glass tape samples. According to obtained results it is possible to conclude that all tested samples are ferroelectrics.

Acknowledgements

This work was supported by the International Science and Technology Center (Projects # A-1591). Author is very gratefull to all project team and to Dr. Rafael Hovhannisyan , Dr. Nikolay Knyazyan and Prof. Heli Jantunen for effective cooperation and fruitful discussions.

Author details

Martun Hovhannisyan*

Address all correspondence to: eni_arm@yahoo.com

Address all correspondence to: raf.hovhannisyan@yahoo.com

http://dx.doi.org/10.5772/52405

Address all correspondence to: martun_h@yahoo.com

«ENI» Institute of Electronic Materials LTD, Armenia

References

[1] The American Ceramic Society & National Institute of Standards and Technology [ACerS & NIST]. (2004). Phase Equilibria Diagrams. *CD-ROM Database, Version 3.0*, 157498215.

[2] Levin, E. M., & Mc Daniel, C. L. (1962). The System Bi_2O_3-B_2O_3. *J. Am.Cer.Soc*, 45(8), 355-360.

[3] Masurin, O. V., et al. (1979). Properties of Glasses and Glass-Forming Melts. Handbook., In Russian, v.III, part 2, L.,, Nauka Press.

[4] Muehlberg, M., Burianek, M., Edongue, H., & Poetsch, C. (2002). $Bi_4B_20_9$ crystal growth and some new attractive properties. *J. Cryst. Growth*, 237, 740-744.

[5] Becker, P., & Bohaty, L. (2003). Linear electro-optic properties of bismuth triborate, BiB_3O_6 (BIBO). *Phys. Chem. Glasses*, 44, 212-214.

[6] Ihara, R., Honma, T., Benino, Y., Fujiwara, T., & Komatsu, T. (2004). Second-order optical nonlinearities of metastable BiBO3 phases in crystallized glasses. *Optical Materials*, 27, 403-408.

[7] Oprea, I. I. (2005). Optical Properties of Borate Glass- Ceramic. *Dissertation zur Erlangung des Grades Doktor der Naturwissenschaften, Osnabruck University, Germany*.

[8] Pottier , M. J. (1974). Mise en evidence d'un compose BiBO3 et de son polymorphisme par spectroscopie vibrationnelle. *Bull. Soc. Chim. Belg.*, 83, 235-238.

[9] Becker, P., Liebertz, J., & Bohatý, L. (1999). Top-seeded growth of bismuth triborate, BiB_3O_6. *J.Cryst.Growth*, 203, 149-155.

[10] Becker, P., & Froehlich, R. (2004). Crystal growth and crystal structure of metastable bismuth ortoborate $BiBO_3$. *Z. Naturforsch. B*, 59, 256-258.

[11] Zargarova, M. I., & Kasumova , M. F. (2004). Liquidus surface of the system ZnO - Bi_2O_3-B_2O_3 projection. *Zh. Neorg. Mater*, In Russian, 26(8), 1678-1681.

[12] Kargin, Yu. F., Zhereb, V. P., & Egorysheva, A. V. (2002). Phase diagram of metastable stats of the Bi_2O_3-B_2O_3 system. *Zh. Neorg. Khim*, 47(8), 1362-1364, In Russian.

[13] Barbier, J., Penin, N., & Cranswick, L. M. (2005). Melilite-Type Borates $Bi_2ZnB_2O_7$ and $CaBiGaB_2O_7$. *Chem. Mater.*, 17, 3130-3136.

[14] Barbier, J., & Cranswick, L. M. (2006). The Non-Centrosymmetric Borate Oxides, $MBi_2B_2O_7$(M=Ca,Sr). *Solid State Chem*, 179, 3958-3964.

[15] Egorisheva, A. V., Skorikov, V. M., & Volodin, V. D. (2008). Calcium Bismuth Borates in the CaO-Bi_2O_3-B_2O_3 system. Zh.Nerg.Mater. In Russian)., 44(1), 76-81.

[16] Kargin, Yu. F., Ivicheva, S. N., Komova, M. G., & Krut'ko, V. A. (2008). Subsolidus Phase Relation in the SrO-Bi_2O_3-B_2O_3 system. *Zh.Nerg.Khim*, 53(3), 474-478, In Russian.

[17] Barbier, J., Davis, L. J. M., Goward, G. R., & Cranswick, L. M. D. (2009). Ab initio structure determination of $SrBi_2OB_4O_9$ by powder X-ray/neutron diffraction and NMR spectroscopy. *Powder Diffr*, 24(1), 35-40.

[18] Levin, E. M., & Mc Murdie, H. F. (1949). The System BaO-B2O3. *J. Res.Nat.Bur.Standards*, 42(2), 131-138.

[19] Levin, E. M., & Ugrinic, G. M. (1953). The System Barium Oxide-Boric Oxide-Silica. *J. Res. Nat.Bur. Stand*, 51, 37-56.

[20] Green, C. H., & Wahler, R. L. (1969). Crystallization of Barium Aluminum Borate Glasses-Rhodium as a Specific Catalyst. *In:Kinetics of reactions in ionic systems. Proc. Intern. Symp. 18-23 IV, New York*, 545-553.

[21] Hubner, K. H. (1969). Ueber die Borate 2BaO•5B_2O_3, tief-BaO•B_2O_3, 2BaO•B_2O_3 und 4BaO•B_2O_3. *Neues Jahrb. Mineral., Monatsch*, 335-343.

[22] Hovhannisyan, R. M. (2006). Binary alkaline-earth borates: phase diagrams correction and low thermal expansion of crystallized stoichiometric glass compositions. *Phys.Chem.Glasses: Eur. J.Glass Sci. Technol. B*, 47(4), 460-465.

[23] Crichton, S. N., & Tomozawa, M. (1997). Prediction of phase separation in binary borate glasses. *J. Non-Crystalline Solids*, 215, 244-251.

[24] Hageman, V. B. M., & Oonk, H. A. J. (1987). Liquid immiscibility in the B_2O_3-MgO, B_2O_3-CaO, B_2O_3-SrO and B_2O_3-BaO systems. *Physics and Chemistry of Glasses*, 28, 183-187.

[25] Klinkova, L. A., Nikolaychik, V. I., Barkovskiy, N. V., & Fedotov, V. K. (1999). Phase relations in the system Ba-Bi-O (20-80 mol% $BiO_{1.5}$) at p_{O2}=0.01, 0,21 and 1 atmosphere. Zh.Neorg. Khim In Russian)., 44(11), 1774-1782.

[26] Mueller, K., Meen, J. K., & Elthon, D. (1999). System BaO-Bi_2O_3 in O_2. *In ACerS & NIST, 2004*.

[27] Shevchuk, A. V., Skorikov, V. M., Kargin, Yu. F., & Konstantinov, V. V. (1985). The system BaO-Bi_2O_3. *Zh.Neorg. Khim*, 30(6), 1519-1522, In Russian.

[28] Witler, D., & Roth, R. S. (2004). System BaO-Bi2O3 in Air,. *in Phase Equilibria Diagrams, CD-ROM Database, A CerS-NITS*.

[29] Barbier, J., Penin, N., Denoyer, A., & Cranswic, L. M. D. (2005). $BaBiBO_4$, a novel noncentrosymmetric borate oxide. *Solid State Science*, 7, 1055-1061.

[30] Egorysheva, A.V, & Kargin Yu, F. (2006). Phase equilibrium in the sub-solidus parts of the Bi_2O_3-BaB_2O_4-B_2O_3 system. *Zh.Neorg. Khim ,In Russian*, 51(7), 1185-1189.

[31] Egorysheva, A.V, Skorikov, V.M, Volodin, V.D, Myslitskiy, O.E, & Kargin, Yu, F. (2006). Phase equilibrium in the BaO-B_2O_3-Bi_2O_3 system. *Zh.Neorg. Khim ,In Russian*, 51(12), 2078-2082.

[32] Bubnova, R. S., Krivovichev, S. V., Filatov, S. K., Egorysheva, A. V., & Kargin, Y. F. (2007). Preparation, crystal structure and thermal expansion if a new bismuth barium borate, $BaBi_2B_4O_{10}$. *Journal of Solid State Chemistry*, 180, 596-603.

[33] Elwell, D., Morris, A. W., & Neate, B. W. (1972). The flux system BaO-B_2O_3-Bi_2O_3. *J. of Crystal Growth*, 16, 67-70.

[34] Hovhannisyan, M. R., et al. (2009). A study of the phase and glass forming diagrams of the BaO-Bi_2O_3-B_2O_3 system. *Phys. Chem.Glasses: Eur. J.Glass Sci. Technol. B*, 50(6), 323-328.

[35] Hovhannisyan, M. R. (2009). Development of low melting sealing glasses on the bismuth borate and tellur molibdate systems basis. PhD Thesis. *State Engineering University of Armenia, Yerevan.*

[36] Hovhannisyan, M. R. (2008). Synthesis of new $BaBi_{10}B_6O_{25}$ compond in BaO-Bi_2O_3-B_2O_3 system. *Chemical J. of Armenia*, 62(2), 28-29.

[37] Hovhannisyan, R. M., et al. (2008). Mutual influence of barium borates, titanates and boron titanates on phase diagram and glass formation in the BaO-TiO2-B2O3 system. *Phys.Chem.Glasses: Eur. J.Glass Sci. Technol. B*, 49(2), 63-67.

[38] Hovhannisyan, R. M. (2010). Melts supercooling-effective way of inorganic systems glassforming and phase diagrams construction. *Proceedings of the II International conference of inorganic chemistry and chemical technology, 13-14th Sept., Yerevan*, 37-39, 978-9-99412-450-3.

[39] Hovhannisyan, R. M. (2011). New generation highly effective electro-and light-active nonlinear oriented tape glass ceramic on the basis of stoichiometric three-coordinated borates. *Final Technical Report of ISTC project # A-1486, Moscow*.

[40] Hovhannisyan, R. M., et al. (2011). Phase diagram, crystallization behavior and ferroelectric properties of stoichiometric glass ceramics in the BaO-TiO_2-B_2O_3 system. *in: Ferroelectrics- Physical Effects, InTech publishing, Croatia*, 49-76.

[41] Hovhannisyan, R. M. (2012). New Lead & Alkali Free Low Melting Sealing Glass Frits & Ceramic Fillers. *Final Technical Report of ISTC project # A-1591, Moscow*.

[42] Barseghyan, A. H., Hovhannisyan , R. M., Petrosyan , B. V., Aleksanyan , H. A., & Toroyan , V. P. (2012). Glass formation and crystalline phases in the ternary CaO-Bi_2O_3-Bi_2O_3 and SrO-Bi_2O_3-B_2O_3 systems. *Phys.Chem.Glasses: Eur. J.Glass Sci. Technol. B, in press*.

[43] International Center for Diffraction Data [ICDD]. (2008). Powder Diffraction Fails, PDF-2 release database,. *Pennsylvania, USA*, 1084-3116.

[44] Sawyer, C. B., & Tower, C. H. (1930). Rochelle Salt as a Dielectric. *Phys. Rev*, 35(3), 269-273.

[45] Imaoka, M., & Yamazaki, T. (1972). Glass-formation ranges of ternary systems. *III. Borates containing b-group elements, Rep. Inst. Ind. Sci. Univ. Tokyo*, 22(3), 173-212.

[46] Janakirama-Rao, Bh. V. (1965). Unusual properties and structure of glasses in the system $BaO-B_2O_3-SrO$, $BaO-B_2O_3-Bi_2O_3$, $BaO-B_2O_3-ZnO$, $BaO-B_2O_3-PbO$, Compt. *Rend. VII Congr. Intern. Du Verre, Bruxelles*, 1(104-104).

[47] Izumitani, T. (1958). Fundamental studies on new optical glasses,. *Rep. Governm. Ind. Res. Inst. Osaka* [311], 127.

[48] Kawanaka, Y, & Matusita, K. (2007). Various properties of bismuth oxide glasses for PbO free new solder glasses. *Proc.XXIth Intern.Congr.on Glass (in CD-ROM), Strasbourg* [I23].

[49] Milyukov, E. M., Vilchinskaya, N. N., & Makarova, T. M. (1982). Optical constants and some other characteristics of glasses in the systems $BaO-Bi_2O_3$ and $La_2O_3-Bi_2O_3-B_2O_3$. Fizika i Khimiya Stekla in Russian)., 8(3), 347-349.

[50] Sarkisov, P. D. (1997). The Directed Glass Crystallization- Basis for Development of Multipurpose Glass Ceramics,. *Mendeleev Russian Chemical Technological University Press, Moscow(In Russian*.

[51] Damjanovic, D. (2005). Hysteresis in Piezoelectric and Ferroelectric Materials,. In: The Science of Hysteresis, Mayergoyz, I & Bertotti, G Elsevier, 0-12480-874-3 , 3, 337-465.

[52] Rawson, H. (1967). Inorganic glass-forming systems. *Academic Press, London & New York*, 312.